Scholars Academic Journal of Biosciences
Abbreviated Key Title: Sch Acad J Biosci
ISSN 2347-9515 (Print) | ISSN 2321-6883 (Online)
Journal homepage: https://saspublishers.com
NIH National Library of Medicine
National Center for Biotechnology Information
NLM ID:101629416
OPEN ACCESS
Chemistry

Seasonal Dynamics and Toxicity of $PM_{2.5}$ in Urban Lahore: Insights from Physicochemical and Oxidative Potential Analysis

Marium Fatima[1], Dr. Shahana Khurshid[1*]

[1]Department of Chemistry and Chemical Engineering, Syed Babar Ali School of Science and Engineering, Lahore University of Management Sciences (LUMS), Lahore, 54792, Pakistan

DOI: https://doi.org/10.36347/sajb.2025.v13i08.013 | **Received:** 17.06.2025 | **Accepted:** 10.08.2025 | **Published:** 18.08.2025

***Corresponding author:** Dr. Shahana Khurshid
Department of Chemistry and Chemical Engineering, Syed Babar Ali School of Science and Engineering, Lahore University of Management Sciences (LUMS), Lahore, 54792, Pakistan

Abstract **Original Research Article**

This study presents a comprehensive physicochemical and toxicological characterization of fine particulate matter ($PM_{2.5}$) collected from August 2024 to April 2025 at the rooftop of the Syed Babar Ali School of Science and Engineering, Lahore University of Management Sciences, using a low-cost size-selective air sampler operating at 15 L/min. Particulate matter was analyzed for morphology and size distribution using scanning electron microscopy (SEM), elemental composition via X-ray fluorescence (XRF), and oxidative potential through an acellular ascorbic acid (AA) depletion assay applied to both water- and methanol-soluble extracts. SEM analysis revealed morphologically diverse particles, including soot agglomerates, carbonaceous chains, and mineral fragments, with aerodynamic diameter shifting from 2.5 µm at 15 L/min to 1.7 µm at 30 L/min. $PM_{2.5}$ concentrations exhibited pronounced seasonal variation, peaking in late autumn and winter (up to ~473 µg/m³) and decreasing to ~58–80 µg/m³ in spring, far exceeding World Health Organization guidelines. Oxidative potential showed similar seasonality, with higher AA depletion rates in winter, particularly in methanol extracts, suggesting dominance of organic-soluble redox-active species such as quinones and PAHs. Weak correlations between $PM_{2.5}$ mass and oxidative potential ($R^2 \leq 0.015$) indicate that chemical composition, rather than particle mass, governs toxicity. Transition metals including Fe, Cu, and Zn were positively associated with $PM_{2.5}$ mass, while Mn, Pb, and as displayed element-specific trends, highlighting source variability. These findings emphasize that health risk assessments and air quality regulations should incorporate compositional metrics alongside mass concentration, particularly in regions with severe seasonal pollution episodes.

Keywords: $PM_{2.5}$, Oxidative potential, Reactive oxygen species, Metal composition, Seasonal variation, Low-cost air sampler, Ascorbic acid assay, Urban air pollution, Morphology analysis.

1. INTRODUCTION

1.1. Background and Significance of Airborne Particulate Matter

Airborne particulate matter (PM) is one of the most common and concerning environmental pollutants in both urban and rural areas worldwide. These complex mixtures of solid particles and liquid droplets suspended in the atmosphere have garnered a lot of scientific attention due to their widespread occurrence and significant impacts on human health, environmental quality, and climate dynamics. Since airborne particulate matter affects practically every aspect of life on Earth, from the air we breathe to the global temperature patterns that sustain ecosystems, its significance cannot be overstated (L. Zhang *et al.,* 2021) (Matter, 2024).

Particle pollution was previously well-known during the Industrial Revolution when areas like Manchester and London were coated with visible smoke and soot from burning coal in homes and businesses. An important turning point in our knowledge of the deadly potential of particulate matter was the infamous London Fog of 1952, which claimed thousands of lives (Matter, 2024). Since then, scientific understanding of particulate matter has changed significantly, revealing its complex composition and extensive impacts that extend far beyond visible air pollution (Matter, 2024; Thompson, 2018).

There are several ways that airborne particulate matter can impact the environment. Localized particles cause material damage, optical impairment, and aesthetic degradation in urban settings(Lippmann *et al.,* 2003). At the regional level, PM can travel hundreds or thousands

Citation: Marium Fatima & Shahana Khurshid. Seasonal Dynamics and Toxicity of $PM_{2.5}$ in Urban Lahore: Insights from Physicochemical and Oxidative Potential Analysis. Sch Acad J Biosci, 2025 Aug 13(8): 1186-1212.

of kilometers from its source, causing transboundary pollution issues that make international relations and regulatory efforts more difficult (Matter, 2024).

Particulate elements like sulfates and black carbon have an impact on the global climate by changing precipitation patterns, cloud formation processes, and the Earth's radiation balance (Matter, 2024). Perhaps the most compelling aspect of particulate matter research is the substantial public health implications it has. Exposure to PM has been frequently linked to increased rates of sickness and mortality, particularly from respiratory and cardiovascular problems, according to numerous epidemiological studies(Matter, 2024; Pope 3rd, 1996).

The World Health Organization estimates that particulate matter is the primary cause of outdoor air pollution, which causes an estimated 4.2 million avoidable deaths annually worldwide(Matter, 2024). This shocking figure emphasizes the tremendous human cost of particle pollution and the urgent need for effective characterization, monitoring, and management techniques (Matter, 2024). The size dimension of particulate matter has a significant influence on its health effects. Particles are categorized based on their aerodynamic dimension; PM_{10} (particles smaller than 10 micrometers) and $PM_{2.5}$ (particles smaller than 2.5 micrometers) are the most often measured percentages(Liu *et al.,* 2020) (Matter, 2024). Fine ($PM_{2.5}$) and ultrafine (less than 0.1 micrometers) particles are particularly hazardous because they can reach the circulation and severely penetrate the respiratory system, where they can result in oxidative stress and systemic inflammation(Matter, 2024) (Matter, 2024). Because particulate matter can elude the body's natural defenses, characterizing its size distribution is essential to understanding exposure pathways and health implications (Matter, 2024).

Recent advancements in analytical techniques have brought attention to the importance of particulates' chemical composition, particularly the presence of metals and reactive oxygen species (ROS), in mediating their toxicity(Matter, 2024). While transition metals like iron, copper, and manganese can catalyze the generation of ROS through Fenton-type reactions, some metals, such as lead, arsenic, and cadmium, are directly detrimental to biological systems(Matter, 2024).

The oxidative potential of particulate matter, which is mostly dependent on its metal content and capacity to generate ROS, is now recognized as a crucial predictor of its health effects, going beyond simple mass-based exposure assessments(Matter, 2024).

The financial cost of particle pollution serves as additional evidence of its significance. Ecological harm, lost productivity, medical costs, and agricultural production losses cost billions of dollars annually. Furthermore, there are serious environmental justice concerns that affect social and economic policy because disadvantaged groups are often disproportionately exposed to particle pollution(Cheema *et al.,* 2024).

1.2. Classification and Size Distribution of Particulate Matter

The aerodynamic diameter of the wide variety of suspended particles that comprise airborne particulate matter (PM) is a key determinant of their atmospheric behavior, residence time, and health impacts. The size distribution of particulate matter is one of the most critical characteristics for understanding its biological interactions and environmental fate, providing vital information for both research and regulatory purposes**.**

The conventional particulate matter classification method is based on size-selective sampling, which replicates the patterns of respiratory deposition in humans. The terms coarse (PM_{10}) and fine ($PM_{2.5}$) refer to particles with aerodynamic diameters less than 10 micrometers (μm) and less than 2.5 μm, respectively. The category of ultrafine particles (UFPs), which have sizes smaller than 0.1 μm (100 nanometres), is growing in significance. This trimodal distribution—coarse, fine, and ultrafine—is the basis for the classification of particulate matter in scientific research and regulatory frameworks worldwide (Harrison & Yin, 2000; Russell & Brunekreef, 2009).

Each size fraction has unique physical and chemical properties that influence its behavior in the environment. Between 2.5 and 10 μm, coarse particles ($PM_{10-2.5}$) are usually the result of anthropogenic activity like mining, construction, and farming as well as mechanical processes like wind erosion, sea spray, and volcanic eruptions. Due to inertial impaction and gravitational settling, these particles typically deposit very close to their emission sources and have shorter air lives, ranging from minutes to hours (Ny & Lee, 2011) (Leung *et al.,* 2014).

The sources and properties of fine particles ($PM_{2.5}$) vary widely. They are mostly caused by combustion processes, such as burning biomass, energy generation, industrial operations, and vehicle emissions (Harrison & Yin, 2000). Additionally, a sizable portion of this component is produced subsequent to atmospheric chemical processes that use ammonia, nitrogen oxides, and sulfur dioxide compounds as precursor gases (Harrison & Yin, 2000; Yamamoto *et al.,* 2014). Due to their small size, fine particles can travel hundreds to thousands of kilometers and remain suspended in the atmosphere for days to weeks, making them major contributors to regional and transboundary pollution. Despite being the smallest fraction of particles in terms of size, ultrafine particles often account for relatively little of the total mass and dominate particle number concentrations. The primary producers of these particles are atmospheric gas nucleation events and high-temperature combustion processes, especially in internal combustion engines(Kero *et al.,* 2021). Their exceptionally small size gives them unique properties, including as high surface area-to-volume ratios, which enhance their capacity to adsorb toxic chemicals and catalyze chemical reactions. Despite their significance for the environment and human health, ultrafine particles are still largely unregulated and not routinely monitored in most air quality networks (Kero & Jørgensen, 2016) (Kero *et al.,* 2021).

1.3. Sources and Emission Patterns of Airborne Particulates

Air quality is significantly impacted at the local, regional, and global levels by the intricate web of man-made and natural sources of airborne particulate matter, as well as by their distinct temporal and geographic emission patterns. To develop effective mitigation strategies, attribute pollution to specific activities, and predict future changes in air quality under different development and climate change scenarios, it is critical to understand these sources and the unique emission fingerprints they produce.

Natural sources contribute significantly to the global particulate matter budget, although their proportional importance varies significantly by place and season. Mineral dust, which is primarily mobilized from dry and semi-arid regions such as the Sahara, Gobi, and Australian deserts, is the largest natural source by mass. Mineral dust is thought to add between 1,000 and 3,000 Tg annually to the atmosphere(Grantz *et al.,* 2003) (Sokhi *et al.,* 2021).

Peak emissions typically happen when it's windy and dry, and they exhibit clear seasonal patterns that are influenced by the weather. Sea spray aerosols, which are created by wave-breaking mechanisms and bubble bursting at the ocean surface, are another significant natural source. Their annual global contribution ranges from 3,000 to 20,000 Tg, with higher emissions occurring in coastal regions and during periods of high wind(Grantz *et al.,,,* 2003). Volcanic eruptions contribute special particulate features to the atmosphere, such as ash particles and secondary sulfate aerosols, which are produced from sulfur dioxide emissions. Despite their rarity, large volcanic eruptions can briefly dominate regional or even global particle budgets. Biogenic sources, such as plant-derived particles (pollen, spores, and plant detritus) and secondary organic aerosols formed from biogenic volatile organic compounds (BVOCs), are additional natural contributions that occur in response to cyclical vegetation cycles (Daellenbach *et al.,* 2020) (Huang *et al.,* 2014) (Grantz *et al.,* 2003).

The bulk of PM budgets in many urban and industrialized areas are today attributed to anthropogenic sources, which have drastically altered the composition and concentration of airborne particles since the Industrial Revolution. The combustion processes, which encompass a broad range of activities, are the most significant group of anthropogenic sources. Fossil fuel combustion in power plants, particularly coal-fired ones, releases large volumes of primary particulates and gaseous precursors that form secondary particles. These emissions typically exhibit seasonal and diurnal patterns that correlate to the energy demand, with characteristic metal profiles that include iron, aluminum, silicon, calcium, and trace elements like arsenic, selenium, and mercury (Grantz *et al.,* 2003) (Dedoussi *et al.,* 2020). Among the modes of transportation that significantly raise urban particle loads are automobiles, ships, and airplanes. Vehicle emissions include fundamental particles from fuel combustion and mechanical processes (tire and brake wear, road dust resuspension) in addition to secondary particles formed from gaseous precursors such as nitrogen oxides. Workweek cycles and commuting hours are correlated with significant diurnal trends in emissions due to traffic. Copper, zinc, antimony, and barium from brake wear, as well as vanadium and nickel from shipping pollutants, are notable examples of elemental fingerprints (Sokhi *et al.,* 2021) (Huang *et al.,* 2014) (Dedoussi *et al.,* 2020).

The particles produced by industrial operations have highly source-specific compositional features. Particles enriched in their target metals and associated elements are released by metallurgical industries; non-ferrous metal smelters release copper, zinc, lead, and arsenic, while steel mills release iron, manganese, and chromium (Pun & Seigneur, 1999). While chemical manufacturing provides a variety of organic and inorganic components, cement-making produces particles that are high in calcium, silica, and aluminum. These emissions frequently exhibit clear time patterns as a result of industrial scheduling (Grover *et al.,* 2006) (Grantz *et al.,* 2003) (Huang *et al.,* 2014).

Burning biomass is a notable example of a hybrid category that incorporates both natural and manmade elements. Burning agricultural trash, controlled forestry fires, and residential wood combustion are examples of deliberate anthropogenic activities, although wildfires are naturally occurring phenomena that are frequently impacted by human land management practices and climate change. Two special chemical markers present in emissions from burning biomass, potassium, and levoglucosan, exhibit clear cyclical patterns linked to agricultural cycles and dry seasons (Pun & Seigneur, 1999) (Grover *et al.,* 2006) (Mukherjee & Agrawal, 2017).

Different geographic conditions produce different emission patterns due to the spatial dispersion of these sources. In urban settings, transportation, residential, and commercial sources are the most common; however, industry also contributes in some locations. The final particle composition reflects this source diversity, with elements like iron, copper, zinc, lead, and vanadium often being elevated relative to background values (Grantz *et al.,* 2003) (Mukherjee & Agrawal, 2017).

Rural areas tend to have lower concentrations, with more contributions from agricultural operations, soil dust, and regional transit, whereas remote locations receive inputs mostly from natural sources and long-distance transmission of anthropogenic emissions (Grover *et al.,* 2006).

1.4. Health Implications of Particulate Matter Exposure

One of the largest environmental risk factors for human health globally is exposure to airborne particulate matter, which can affect the respiratory, cardiovascular, neurological, and metabolic systems. The health impacts of particulate matter exposure have been extensively established through toxicological research, clinical investigations, and epidemiological studies. These investigations have shown complex biological processes and dose-response interactions that are much beyond the traditional understanding of air pollution as simply a respiratory irritant.

The consequences of particle pollution on the respiratory system are the most evident. An increase in ER visits and hospitalizations for ailments like respiratory infections, flare-ups of chronic obstructive pulmonary disease (COPD), and asthma episodes is linked to brief increases in ambient particle concentrations (Manisalidis *et al.,* 2020) (Matter, 2024).

These acute reactions are frequently accompanied by bronchial hyperresponsiveness, increased mucus production, and airway inflammation. By changing the structure of lung tissue and disrupting pulmonary defense mechanisms, long-term particle exposure speeds up the deterioration of lung function, results in COPD, and makes people more vulnerable to respiratory infections (Matter, 2024) (Anderson *et al.,* 2012; Manisalidis *et al.,* 2020). Particulate matter has been shown to have an impact on the central nervous system and may be connected to neurodevelopmental and neurodegenerative diseases (Pun & Seigneur, 1999) (Anderson *et al.,* 2012).

The size and composition of particulate matter have a significant impact on its health effects. Finer particles penetrate further into the respiratory system as $PM_{2.5}$ reaches the alveolar region and ultrafine particles may enter the circulation (Pryor *et al.,* 2022) (Anderson *et al.,* 2012) . This size-dependent deposition pattern helps to explain the higher associations observed between exposure to fine particles and systemic health effects outside of the respiratory system. Because transition metals like iron, copper, and zinc stimulate Fenton-type processes that generate reactive oxygen species (ROS), the metal content largely determines the toxicity of particulates (Manisalidis *et al.,* 2020) (Pryor *et al.,* 2022). These ROS result in oxidative stress at the cellular level, which harms proteins, lipids, and DNA and triggers inflammatory responses that are the primary cause of numerous detrimental health effects (Pryor *et al.,* 2022).

According to public health, there are significant societal costs associated with the harmful health effects of particle exposure. According to estimates from the Global Burden of Disease study, exposure to ambient particulate matter is one of the main environmental risk factors in the globe, causing about 4.2 million avoidable deaths per year (Trejo-González *et al.,* 2019) .

An estimated hundreds of billions of dollars are spent each year on healthcare, lost productivity, and diminished quality of life. Even while many wealthy countries have made great strides in lowering particle emissions, the ongoing urbanization and industrialization in emerging countries will make particle pollution a serious global health risk for decades to come. This emphasizes how crucial it is to carry out additional research on the intricate relationships between particles (Trejo-González *et al.,* 2019) (Guillerm & Cesari, 2015).

1.5. Reactive Oxygen Species (ROS) in Airborne Particulates:
Formation and Measurement

Reactive oxygen species (ROS) associated with airborne particulate matter are a key determinant of toxicity and a pathway linking exposure to adverse health effects. These highly reactive substances include the superoxide anion (O_2^-), hydrogen peroxide (H_2O_2), hydroxyl radical (•OH), and singlet oxygen ($^1O_2$) (Z.-H. Zhang *et al.,* 2021) (Murphy *et al.,* 2022). Each has distinct biological implications and reactivity patterns. Understanding the production processes, measurement methods, and effects of ROS in particulate matter has been a key focus of research on atmospheric chemistry and inhalation toxicity.

Although ROS are generated in airborne particulates in a variety of ways, they can be broadly classified into two groups: extrinsic (made by contact with biological systems) and intrinsic (particle-bound) (Shahpoury *et al.,* 2024) (Murphy *et al.,* 2022) (Z.-H. Zhang *et al.,* 2021) . Intrinsic ROS, which are present on particle surfaces or in the particle matrix, can be measured using particle extracts (Shahpoury *et al.,* 2024). These substances are produced by combustion, atmospheric aging, and photochemical reactions. High-temperature combustion naturally produces ROS through radical generation, particularly in emissions from burning biomass, vehicles, and industrial facilities (Vörösmarty *et al.,,,* 2023). Once in the air, particles experience photochemical aging as a result of interactions between sun radiation and adsorbed organic molecules. Through photosensitization events involving polycyclic aromatic hydrocarbons (PAHs) and other photoactive components, this interaction frequently leads to the generation of reactive oxygen species (ROS) (Z.-H. Zhang *et al.,* 2021) (Vörösmarty *et al.,* 2023).

Metal-mediated ROS generation is one of the most significant pathways in particulate matter toxicity. Transition metals like iron, copper, manganese, and chromium can participate in redox cycling reactions that generate ROS through Fenton and Haber-Weiss chemistry (Lelieveld *et al.,* 2021). These reactions between hydrogen peroxide and reduced metal ions produce hydroxyl radicals, one of the most reactive and dangerous ROS. Iron, particularly in its Fe^{2+} state, has a significant tendency to produce ROS, as demonstrated by the reaction $Fe^{2+} + H_2O_2 \rightarrow Fe^{3+} + \bullet OH + OH^-$ (Lelieveld *et al.,* 2021) (Li *et al.,* 2008). The subsequent reduction of Fe^{3+} back to Fe^{2+} by cellular reductants or other particulate components enables continuous ROS production in a catalytic cycle (Li *et al.,* 2008).

Measuring ROS in particulate matter presents significant methodological challenges due to their intrinsic instability and reactive nature. The two primary types of methods are cellular and acellular techniques, each with special advantages and disadvantages (Brown *et al.,* 2019) (Shahpoury *et al.,* 2024). In acellular assays, particles are often removed into solution and their capacity to oxidize target molecules or generate ROS is assessed. The dichlorofluorescein (DCFH) assay measures the oxidation of non-fluorescent DCFH to fluorescent DCF by various ROS and provides a wide indication of oxidative potential (Brown *et al.,* 2019) (Shahpoury *et al.,* 2024).

The dithiothreitol (DTT) assay measures the capacity of particulate matter to transfer electrons from DTT to oxygen, generating superoxide and, subsequently, more ROS (Lelieveld *et al.,* 2021). This test is extremely sensitive to some metals and redox-active chemical compounds. Electron spin resonance (ESR) spectroscopy with spin trapping agents offers more specific identification of radical species by capturing transient radicals as more stable adducts, enabling characterization of specific ROS produced by different particulate fractions(Lakey *et al.,* 2016).

1.6. Metal Composition in Particulate Matter: Common Elements and Their Origins

Airborne particulate matter's metal content is an important factor that affects its toxicological characteristics and offers useful data for source apportionment investigations. Despite making up just 1% to 5% of particulate matter in urban settings, metals are very important components for characterization due to their biological reactivity, environmental durability, and unique source signals. Finding the causes of pollution and possible health hazards is made easier by knowing the origins, distribution, and speciation of metals in particulate matter (Soleimanian *et al.,* 2019).

Iron (Fe), silicon (Si), calcium (Ca), titanium (Ti), and aluminum (Al) are among the elements that typically make up the majority of the metal mass percentage of coarse particulate matter. The primary sources of these components are construction, road dust resuspension, agricultural operations, and natural soil dust entrainment (Soleimanian *et al.,* 2019) (Alghamdi, 2016). Their relative abundances in particulate matter often approximate their crustal ratios, even though urban areas may show enrichment in calcium from construction materials and iron from anthropogenic sources. The most prevalent chemical forms in particulate matter are the oxides of these elements, such as SiO_3, CaO, TiO_2, FeO_3, and AlO_3. After inhalation, their solubility may rise in the acidic lung milieu, but it is typically limited in ambient conditions (Alghamdi, 2016).

Transition metals including vanadium (V), chromium (Cr), manganese (Mn), iron (Fe), nickel (Ni), copper (Cu), and zinc (Zn) in particulate matter typically show significant man-made enrichment in urban and industrial contexts, despite their natural and man-made origins (Alghamdi, 2016) (Choi *et al.,* 2022). Burning residual oil for shipping and heating is the main source of nickel and vanadium, which are sometimes found in a unique ratio (Choi *et al.,* 2022). Chromium and manganese are found in emissions from metallurgical industries, particularly those involved in the production and processing of steel (Choi *et al.,* 2022) (Potter *et al.,* 2021). Copper, zinc, and antimony show strong associations with non-exhaust traffic emissions, particularly brake wear, with copper content in brake pads ranging from 1-15% by weight in many formulations (Alghamdi, 2016). Some heavy metals, such as lead (Pb), cadmium (Cd), and mercury (Hg), are especially problematic due to their recognized toxicity profiles and lack of biological activity in humans. Historical trends for these elements show shifting emission patterns, with lead concentrations significantly declining when leaded gasoline was phased out globally starting in the 1970s (Potter *et al.,* 2021) (Alghamdi, 2016).

1.7. Oxidative Potential of Metals in Airborne Particulates

The oxidative potential of airborne particulate matter—its capacity to generate reactive oxygen species (ROS) and induce oxidative stress in biological systems—represents a significant driver of toxicity that goes beyond traditional mass-based exposure assessments. This paradigm states that metals participate in redox cycling reactions, catalyze the creation of highly reactive radical species, and transport electrons, all of which contribute to oxidative potential.

Transition metals have important relationships with oxidative potential due to their variable oxidation states and their capacity for electron transport activities. Iron, the most common redox-active metal in most particulate samples, is important because of its role in Fenton chemistry, which creates highly reactive hydroxyl radicals (•OH) when ferrous iron (Fe^{2+}) reacts with hydrogen peroxide (H_2O_2). This reaction proceeds as follows:

$$\mathbf{Fe^{2+} + H_2O_2 \rightarrow Fe^{3+} + \bullet OH + OH^-}$$

(Campbell *et al.,* 2023). Catalytic cycling and continual ROS production are made possible by the regeneration of Fe^{2+} from Fe^{3+} through reactions with superoxide (O_2^-) or biological reductants like glutathione or corbate. Its oxidative potential is greatly affected by iron speciation; soluble iron oxides (Fe^{2+}) are substantially more active than insoluble iron oxides (Fe^{3+}) (Liu *et al.,* 2018).

Copper has an even higher mass-normalized oxidative potential than iron in a number of test methods, although having a generally lower concentration in particulate matter. As copper alternates between the Cu^+ and Cu^{2+} oxidation states (Liu *et al.,* 2018) (Campbell *et al.,* 2023) (Charrier & Anastasio, 2012). Additionally, copper has a strong affinity for specific regions of proteins and DNA, which could lead to the generation of localized ROS and subsequent biomolecular damage. Copper accelerates the production of hydroxyl radicals by reducing Fe^{3+} to the more reactive Fe^{2+} form. Oxidative potential is further increased by these copper-iron synergistic interactions (Charrier & Anastasio, 2012) (Campbell *et al.,* 2023).

Other transition metals like manganese, chromium, vanadium, and nickel all contribute to oxidative potential in different ways. Manganese can boost iron's oxidative potential and aid in the synthesis of superoxide through synergistic interactions. Chromium, particularly in its hexavalent form [Cr(VI)], induces oxidative stress through intracellular reduction to Cr(V) and Cr(IV) intermediates, which generate ROS while the metal is reduced to Cr(III). Vanadium compounds, especially vanadium pentoxide (V_2O_5), can generate reactive oxygen species (ROS) when they are reduced by cellular antioxidants and then react with molecular oxygen. Nickel chemicals induce oxidative stress and oxidative damage to cell macromolecules by inhibiting antioxidant defense mechanisms (Liu *et al.,* 2018) (Charrier & Anastasio, 2012).

The amount that each metal contributes to the total particulate oxidative potential varies greatly depending on the type of source, the environment, and the analytical method. Strong correlations between copper content and oxidative potential are commonly found in urban particulate matter, particularly near highways where emissions from brake wear that contain 1–15% copper by weight greatly increase ambient concentrations. Industrial emissions from steel plants have source-specific oxidative potential fingerprints, meaning that the particles they produce have a higher potential to generate hydroxyl radicals due to their high iron and manganese content (Weber *et al.,* 2021) (Charrier & Anastasio, 2012). Coal combustion pollutants contain a number of components, including iron, chromium, and arsenic, which collectively give them their oxidative properties (Weber *et al.,* 2021) (Charrier & Anastasio, 2012).

Significant progress in analytical methods for assessing metal-driven oxidative potential has made it possible to characterize these complex relationships in greater detail. Acellular tests like the dithiothreitol (DTT) assay, which measures the capacity of particulate components to transfer electrons from DTT to oxygen-forming superoxide, show strong reactivity to copper and other redox-active metals (Charrier & Anastasio, 2012). The ascorbic acid (AA) depletion assay, which gauges consumption of this antioxidant, is very susceptible to iron and copper. Electron spin resonance combined with spin trapping techniques allows for more accurate identification of radical species generated by different metals (Charrier & Anastasio, 2012) (Campbell *et al.,* 2023)

Combining metal speciation data with oxidative potential measurements is a growing technique for more precise risk assessment. Advanced techniques like X-ray absorption spectroscopy (XAS) and X-ray photoelectron spectroscopy (XPS) provide in-depth information on the metal oxidation states and chemical environments found in particulate matter. These techniques demonstrate that particulate oxidative activity is directly related to redox-active metal species in bioavailable forms, not merely the total metal content when combined with oxidative potential tests (Charrier & Anastasio, 2012) (Campbell *et al.,* 2023).

1.8. ROS Generation Mechanisms in Particulate Matte

The generation of ROS by metals is one of the most significant processes in particulate matter toxicity. Transition metals with varying oxidation states, such as iron, copper, manganese, and chromium, can participate in electron transfer processes that transform comparatively stable oxygen molecules into more reactive ones. The Fenton reaction, in which ferrous iron (Fe^{2+}) reacts with hydrogen peroxide to produce hydroxyl radicals ($Fe^{2+} + H_2O_2 \rightarrow Fe^{3+} + \bullet OH + OH^-$), best illustrates this mechanism (Charrier & Anastasio, 2012) (Tacu *et al.,* 2021) (Mazzoli-Rocha *et al.,* 2010) . The hydroxyl radical generated in this reaction is one of the most potent oxidizing species present in biological systems, capable of damaging proteins, lipids, and DNA through hydrogen abstraction and addition processes (Mazzoli-Rocha *et al.,* 2010).

Photochemical reactions have a major impact on the generation of ROS, particularly for particles containing photoactive components. When exposed to sunlight, some chemical molecules present in particulate matter, including polycyclic aromatic hydrocarbons (PAHs) and quinones, can function as photosensitizers. They have the ability to absorb photon energy and transform it into electrons to produce superoxide or singlet oxygen (O_2) from molecular oxygen. These ROS, which are created by photochemistry, can damage biomolecules directly or initiate chain reactions that produce more reactive species. Because the photochemical activity of particulate matter varies spectrally based on the absorption properties of its constituents and diurnally with solar intensity, temporal patterns in oxidative potential may not be accurately connected with changes in mass concentrations (Mazuryk *et al.,* 2020) (Li *et al.,* 2008).

1.9. Analytical Techniques for Characterization of Particulate Matter

Particulate matter (PM) must be characterized using sophisticated analytical techniques in order to fully comprehend its intricate physical and chemical characteristics. Over the past few decades, these methods have advanced dramatically, allowing scientists to get a deeper understanding of the characteristics of these common air pollutants and their effects on human health and the environment. The international regulatory standard and the fundamental method for figuring out PM mass concentrations is gravimetric analysis (Sousan *et al.,* 2022) (Zhu *et al.,* 2011).

This technique entails gathering particles on pre-weighed filters and computing the mass increase following sampling in an environment with controlled humidity and temperature. Using microscopy techniques can help us better understand the morphology and microstructure of PM. Particle sizes and shapes can be imaged using Energy Dispersive X-ray Spectroscopy (EDX) and Scanning Electron Microscopy (SEM), which also provides information on elemental composition (Jellal *et al.,* 2024).

Spectroscopic methods have revolutionized the analysis of PM composition. Because it allows for the non-destructive analysis of components ranging from sodium to uranium, X-ray fluorescence (XRF) spectroscopy is highly useful for investigating metals in PM. Inductively Coupled Plasma Mass Spectrometry (ICP-MS) provides exceptional sensitivity for trace metal detection, detecting amounts in the parts-per-trillion level (Jameson *et al.,* 2022). Technologies for continuous and real-time monitoring have become essential resources for temporal research. Continuous measurements of the size-resolved chemical composition of non-refractory submicron particles are made possible using Aerosol Mass Spectrometers (AMS) (Jeong *et al.,* 2011).

For elemental characterization of particulate matter, Inductively Coupled Plasma Optical Emission Spectroscopy (ICP-OES) is a crucial analytical technique. By subjecting sample extracts to a high-temperature plasma, typically between 6,000 and 10,000 K, the technique atomizes and excites the constituent elements. Upon relaxation, these excited atoms and ions emit electromagnetic radiation at characteristic wavelengths, with emission intensities proportional to elemental concentrations (Nelms & Kutscher, 2022).

Particulate matter analysis with ICP-OES often requires acid digestion of filter-collected samples using combinations of strong acids (HNO_3, HCl, HF, and H_2O_2) under controlled temperature and pressure settings (Tyler & Yvon, 1995). Microwave-assisted digesting systems have greatly improved the efficiency and reproducibility of this preparation phase. For most metals, the method has detection limits in the low µg/L region, enabling the identification of both significant constituents and trace elements in a single analytical run. Its linear dynamic ranges extend many orders of magnitude (Blades, 2022).

1.10. Sampling Methodologies and Challenges

Accurate characterization of particulate matter (PM) fundamentally depends on robust sampling methodologies that can effectively capture the complex and dynamic nature of atmospheric aerosols. Traditional filter-based sampling remains the most widely employed approach for collecting particulate matter. High-volume samplers, operating at flow rates of 100-1000 L/min, enable the collection of sufficient mass for comprehensive chemical analysis but may introduce artifacts due to reactive gas adsorption and volatile component losses (Moore *et al.,* 2015) (Patel & Aggarwal, 2022). Medium-volume samplers (15-40 L/min) and low-volume samplers (1-10 L/min) offer greater flexibility for field deployment while maintaining reasonable collection efficiency (Moore *et al.,* 2015). These systems typically employ various filter media, including quartz fiber, Teflon membrane, and nylon filters, each with specific advantages for particular analytical techniques. Quartz filters withstand high temperatures necessary for carbon analysis but may adsorb organic vapors, while Teflon filters provide excellent gravimetric stability but are incompatible with certain chemical analyses (Chen & Liu, 2023) (Offor *et al.,* 2016) (Moore *et al.,* 2015).

Size-selective inlets represent a critical component of PM sampling systems, enabling the collection of specific aerodynamic diameter fractions relevant to regulatory standards and health impact assessments. PM_{10} cyclones and impactors collect particles with aerodynamic diameters less than 10 µm, while $PM_{2.5}$ selective inlets target the fine fraction below 2.5 µm (Patel & Aggarwal, 2022) (Offor *et al.,* 2016). The ultrafine fraction ($PM_{0.1}$) presents particular sampling challenges due to diffusion losses and charging effects, requiring specialized collection approaches. Cascade impactors further enable size-resolved sampling across multiple stages, providing valuable information about size-dependent composition differences, though flow rate limitations and particle bounce effects can compromise their accuracy (Moore *et al.,* 2015) (Chen & Liu, 2023).

1.11. Regulatory Standards and Monitoring Approaches

The global air quality guidelines issued by the World Health Organization (WHO) serve as a benchmark for national regulatory regimes. The WHO's 2021 revised guidelines drastically reduced recommended limits for $PM_{2.5}$ to a 24-hour mean of 15 µg/m³ and an annual mean of 5 µg/m³ due to mounting evidence of health effects at previously safe amounts (Organization, 2021b) (Hoffmann *et al.,* 2021).The US Environmental Protection Agency (EPA) establishes the National Ambient Air Quality Standards (NAAQS) for PM in accordance with the Clean Air Act. Currently, PM2.5 (35 µg/m³, 24-hour; 12 µg/m³, annually) and PM_{10} (150 µg/m³, 24-hour) are both controlled, and compliance is evaluated using a particular reference technique that employs gravimetric filter analysis (Organization, 2021b) (Organization, 2021a).

Mandatory limit restrictions for member states are established by the European Union's ambient air quality rules. These include $PM_{2.5}$ (25 µg/m³, annually) and PM_{10} (50 µg/m³, 24-hour, not to be exceeded more than 35 times per year; 40 µg/m³, annually) (Organization & Organization, 2021). Instead of only aiming for absolute levels, the EU framework's exposure reduction strategy for $PM_{2.5}$ aims for percentage reductions in average urban background concentrations.

Asian countries face particular challenges in controlling PM because of their rapid industrialization and urbanization. China has gradually improved its ambient air quality restrictions. However, they are still less stringent than WHO guidelines. There has been a significant improvement in the present $PM_{2.5}$ levels (35 µg/m³, annually; 75 µg/m³, 24-hour). Implementation problems with India's National Ambient Air Quality Standards, which set $PM_{2.5}$ levels at 40 µg/m³ (annual) and 60 µg/m³ (24-hour), include a lack of enforcement capacity and monitoring infrastructure (Esworthy, 2013).

2. LITERATURE REVIEW

2.1. Metal Composition in $PM_{2.5}$

(Lindberg & Turner, 1988) The transit and retention of trace metals in wooded watersheds have been clarified by research on metal deposition and streamflow outputs. Between 1976 and 1982, four deciduous woodland watersheds in the southeast United States were studied to examine the imports of Cd, Mn, Pb, Zn, and Al through wet and dry deposition as well as the streamflow outputs of these elements. Despite the fact that air intakes were the same at each site, metal concentrations differed by factors of 1.1 to 2.2, suggesting that deposition methods varied geographically. Metal precipitation levels were comparable to those in continental, rural regions, and rainwater metal concentrations displayed significant spatial and temporal trends. Seasonal fluctuations revealed that summer concentrations were higher than winter concentrations, despite the fact that concentrations were normally lower in farther-flung places.

Significantly, between 1976–1977 and 1981–1982, levels of Cd and Pb in both wet and dry deposition decreased, most likely as a result of modifications in air emissions. While Cd, Pb, and Zn were enriched above normal soil levels, indicating human inputs, enrichment factor analysis showed that Mn came mostly from soil sources. Furthermore, factor analysis showed that although both factors affected Pb, soil components primarily caused Cd deposition, while fine aerosol components influenced both Al and Mn. Wet deposition accounted for 54–85% of the total intake of Cd, Pb, and Zn, while dry deposition was the main source of Mn and Al. Deposition patterns also differed by metal. The retention rates of deposited metals were very high, with 8–29% of Cd, 8–34% of Zn, and just 2% of Pb transported by streamflow, although Mn and Al had lower retention rates, with a net loss at some sites. The substantial impacts of site-specific factors, such as bedrock geology, organic carbon content, stream pH, and hydrologic conditions, on the export of these metals brought to light the complex linkages governing metal mobility and retention in watershed ecosystems.

(Ruijrok *et al.,* 1995) This research assesses the current understanding of dry deposition of particles with a focus on the consequences for Europe. Physical characteristics, general source factors, and particle concentration data are considered. The modeling methods currently used to estimate the dry deposition of course and small particles are evaluated. The uncertainties and limitations of these models are highlighted. Measurements of small- and large-particle deposition using various techniques are summarized and their limits discussed. Finally, with an emphasis on Europe, the effects of the scale features of particle dry deposition are explored. The overall conclusion is that the lack of experimental and theoretical knowledge of particle dry deposition compromises the ability to make reliable estimations of deposition fluxes over Europe.

(Watson *et al.,* 2002) Receptor models evaluate contributions from various PM sources using multivariate measures of particle chemical and physical characteristics. Receptor models complement source models that predict concentrations based on transport meteorology and emissions inventories. Enrichment factor, chemical mass balance, multiple linear regression, eigenvector, edge detection, neural network, aerosol evolution, and aerosol equilibrium models are used to address particle air quality challenges, as evidenced by more than five hundred citations of its theory and application. Several of these components have been reduced in source emissions to the point where more precise measurements of carbon fractions, particularly organic compounds, can be employed, even if TSP, PM_{10}, and $PM_{2.5}$ were previously assigned to different source types based on elements, ions, and carbons.

This is so because observables, locations, and time periods are not usually the focus of compliance monitoring networks. By using measurements from existing networks to create conceptual models, it might be able to optimize the necessary monitoring network. The framework for using receptor models to solve air quality problems consists of the following steps: developing a conceptual model, identifying potential sources, characterizing source emissions, obtaining and analyzing ambient PM samples for major components and source markers, verifying source types with multivariate receptor models, quantifying source contributions using the chemical mass balance, estimating profile changes and the limiting precursor gases for secondary aerosols, and balancing receptor modeling results with source models, emissions inventories, and other factors.

(Abdul-Wahab, 2004) The Sohar Industrial Estate (SIE) and a residential neighborhood in the Oman case study location were the two districts where total suspended particle matter (TSP) was gathered. While the TSP gathered from the residential sector originated from 12 homes, the TSP gathered from SIE came from 19 distinct industrial activities. The samples contained nine different heavy metals: molybdenum, cadmium, vanadium, nickel, lead (Pb), zinc (Zn), copper (Cu), manganese (Mn), and chromium (Cr). The results were used to identify the source classes responsible for the TSP and heavy metal concentrations in the atmospheres of the two districts. By using principal component analysis on the TSP and heavy metal concentrations for every district, the number of main components was ascertained. The second one (machine industries, vehicle construction, and the production of black and galvanized iron pipes) differed the greatest in terms of Cr, Pb, and Zn. Lead and zinc made up the third component, which most likely came from vehicle tire wear or municipal burning. However, according to the village's findings, the industrial site was contaminating the village's air with Cu, Cr, Pb, nickel, and Mn, and the majority of the variance in the data could be explained by just one factor.

(Lee & Hieu, 2011) This study looked for seasonal variations in particulate matter (PM) mass concentrations and the heavy metal compositions of $PM_{2.5}$ and PM_{10}, which were gathered from a typical urban residential area in Ulsan, Korea. PM was measured during the spring and summer of 2009. The mean $PM_{2.5}$ levels were 23.2 µg/m3 in the spring and 18.1 µg/m3 in the summer. The mean PM10 values were 45.9 µg/m3 in the spring and 33.2 µg/m3 in the summer. Summer PM concentrations are lower than spring PM concentrations because of the increased rainfall and precipitation. Heavy elements Fe, Zn, Cd, Mn, Pb, Cu, Cr, and Ni were measured in airborne PM. All of the metals in $PM_{2.5}$ and PM_{10} have higher concentrations in PM2.5 than in PM10, with the exception of Cr in PM_{10}, which shows similar values in spring and summer. Seasonal fluctuations in metal concentrations may be caused by different wind directions, some of which pass through areas with traffic or industry. According to heavy metal enrichment factor analysis, there was a significant enrichment of Cd, Zn, Pb, and Cu. Principal component analysis was used to identify the main sources of road dust (traffic and soil) and industrial emissions at the sampling site for the heavy metals in $PM_{2.5}$ and PM_{10}.

(Khodeir *et al.,* 2012) For the first time, this study looks closely at the origins and composition of particulate matter in Saudi Arabia that has aerodynamic dimensions of ≤2.5 µm ($PM_{2.5}$) and ≤10 µm (PM_{10}). A multi-week sampling campaign was conducted in numerous Jeddah areas between June and September 2011. The samples collected were assessed using X-ray fluorescence (XRF).

The mean mass concentrations were 28.4 ± 25.4 µg/m³ for PM2.5 and 87.3 ± 47.3 µg/m³ for PM_{10}, with notable geographical and temporal heterogeneity. On average, the PM2.5 to PM_{10} ratio was 0.33. To identify the four and five primary source groups that contribute to $PM_{2.5}$ and PM_{10}, respectively, the chemical composition data was evaluated using factor analysis with Varimax orthogonal rotation. Both size fractions shared three primary sources: (1) re-suspended soil, which is rich in silicon, calcium, iron, and aluminum; (2) heavy oil combustion, which is indicated by a high concentration of nickel and vanadium; and (3) a mixed industrial source. Regressing PM mass concentrations against the factor scores allowed for the quantification of source contributions, which revealed that re-suspended soil and oil combustion were responsible for 77% of PM_{10} mass and 82% of $PM_{2.5}$ mass. Marine aerosols also contributed to PM10, while (4) vehicle emissions containing lead, bromine, and selenium and (5) another industrial source affected $PM_{2.5}$.

(Sharma *et al.,* 2003) An Air Quality Index (AQI) is recommended for the City of Delhi to help with public communication and data interpretation. The maximal operator idea, which uses the largest value of the subindices (of each pollutant) as the overall AQI, is used to determine the overall AQI. The mathematical functions for determining subindices are proposed after considering USEPA health standards and Indian air quality rules (Federal Register, December 9, 1998). The pollutants that are included in the index include suspended particle matter (SPM), CO, NO_2, PM_{10}, O_3, and SO_2.(Querol *et al.,* 2000) The collapse of the storage lake dam of the Boliden corporation left the Guadiamar Valley, north of the Doñana Natural Park in southwest Spain, blanketed in a layer of pyrite-rich sludge. The primary focus of this work is the physico-chemical characterization of suspended particles during times of elevated air particulate matter, primarily caused by soil reclamation activities. Comprehensive air particle sampling was conducted at two monitoring stations, one in Aznalcázar and one in the Guadiamar Valley, between May 20 and December 27. During the peak reclamation season (July–August 1998),

Aznalcázar's daily mean concentrations of total suspended particles (TSP) reached 191.2 µg/m³, with a maximum recorded value of 490 µg/m³. As reclamation activities continued, TSP levels gradually dropped, reaching roughly 90 µg/m³ in September–October and 40 µg/m³ by November–December.Extremely high levels of major and trace elements were found at both sampling locations. Before gradually decreasing in the fall and winter, ambient air levels of these components rose by two orders of magnitude in July and August compared to May and June. Average daily concentrations for Ag, Cd, Sn, and Tl in Aznalcázar between July and August were roughly 2 ng/m³; Ni was 10 ng/m³; Mn was 100 ng/m³; As and Cu were 200 ng/m³; and Pb and Zn were 450 ng/m³. Concentrations were up to three times greater in the Guadiamar Valley, where most of the soil reclamation work was done, than in Aznalcázar. In terms of particle size fractions, As, Cd, Co, Pb, Sb, Se, and Tl concentrations in PM2.5 and PM10, respectively, accounted for around 20–48% and 80–90% of TSP. Each of these elements had a distinct water-soluble fraction in TSP: Ni, As, Zn, and Cu exhibited moderate solubility (8–10%), while Cd, Co, Tl, Mn, and Se demonstrated high solubility (27–92% of total content). Pb, Sb, and Cr were primarily insoluble, accounting for less than 4% of their total content in the extractable fraction.

(Harper *et al.,* 1983) The settings for ultrasonic extraction of trace elements from airborne particles collected on glass-fiber filters using high-volume samplers were optimized using a simplex search technique. For 13 elements, the improved approach produced quantitative findings with accuracy over 95% and precision within 10%. In addition, it turned out to be safer, quicker, and more economical than traditional boiling-acid extraction methods. This approach has been approved by the Environmental Protection Agency (EPA) as a legitimate substitute for the conventional lead reference procedure. Inductively coupled plasma optical emission spectrometry, atomic absorption spectrophotometry, and neutron activation analysis were used to analyze split samples in order to validate the procedure. These were used with National Bureau of Standards Standard Reference Material No. 1648, synthetic spikes, and actual particle samples.

2.2. Ascorbic Acid Assay in $PM_{2.5}$ Oxidative Potential Studies

The oxidative potential (OP) of particulate matter (PM) is a critical metric for assessing the health impacts of PM, particularly in environmental and occupational environments. OP reflects PM's capacity to induce oxidative stress, which is linked to several detrimental health impacts. Recent studies have employed the ascorbate assay (OPAA) to measure OP, and the findings indicate a robust association between PM characteristics and health outcomes. The following sections elaborate on the key findings about OPAA and its implications.

(Dubey *et al.,* 2024) The oxidative potential (OP) of $PM_{2.5}$ was assessed in this study using the ascorbic acid (AA) assay, an acellular method for determining the redox activity of particulate matter. The AA assay, which measures the ascorbic acid depletion that follows exposure to $PM_{2.5}$, demonstrates the presence of redox-active species that are capable of producing reactive oxygen species (ROS). The intrinsic OPAA (OPAAm) levels in Bengaluru were the highest, with a mean value of 1.62 ± 0.34 nmol/min/m³. These levels were approximately four and six times higher than those in Delhi (0.41 ± 0.21 nmol/min/m³) and Mumbai (0.26 ± 0.14 nmol/min/m³), respectively. The coefficient of divergence (COD) for extrinsic OPAA (OPAAv), which was 1.5 times greater than that of OPDTTv, also demonstrated notable heterogeneity. This implies that there is greater regional variability in the oxidative potential based on AA. The highest OPAAv values, which varied from 5.13 to 4.22 nmol/min/m³, were found in high-traffic regions of all three cities. Additionally, OPDTTv levels in Mumbai were comparable in the summer and winter, suggesting that $PM_{2.5}$ toxicity was significantly influenced by primary traffic aerosols. The study found that water-soluble organic carbon (WSOC), vanadium (V), and cobalt (Co) are the primary contributors to ROS activity. These findings demonstrate the role that traffic-related pollutants play in increasing oxidative stress in urban environments by demonstrating how $PM_{2.5's}$ oxidative potential is influenced by its chemical composition and emissions from certain sources.

(Shen *et al.,* 2021) Ascorbic acid, one of the most prevalent antioxidants in the lung, most likely plays a significant function in regulating the biological responses triggered by particle air pollution. It is a highly redox-active compound that interacts complexly with oxidants like hydroxyl radicals and redox-active transition metals like iron and copper. Even though the underlying chemistry has been well studied, there are still notable discrepancies in reported stoichiometries, methods, and reaction rates, particularly with regard to transition metal interactions. This study creates a chemical kinetics model, applies data from seven experimental datasets, and integrates the body of existing literature to constrain significant processes involving iron and copper reactions and finally yield usable rate constants. The results demonstrate that micromolar amounts of iron (III) and copper (II) deplete ascorbic acid (both AH_2 and AH^-) more effectively than reactive oxygen species. These reactions are catalytic rather than simply redox, and proceed with unit stoichiometries indicated by Fe(III)/Cu(II) + AH_2/AH^- + O_2 → Fe(III)/Cu(II) + H_2O_2 + products. With rate constants of 5.7×10^4 and 4.7×10^4 M^{-2} s^{-1} and 7.7×10^4 and 2.8×10^6 M^{-2} s^{-1}, respectively, it has been demonstrated that Fe(III) and Cu(II) react with AH_2/AH^-.

(Utinger *et al.,* 2023) Epidemiological studies have frequently linked exposure to ambient particulate matter (PM) to a number of detrimental health effects. However, little is understood about the fundamental mechanisms behind particle toxicity as well as the specific chemical and physical characteristics of particles that contribute to these detrimental health effects. Numerous studies have shown that the oxidative potential (OP) of aerosol particles is a critical indicator of their toxicity. The ability of an aerosol to release reactive oxygen species (ROS) and exhaust the body's antioxidant stores is referred to as OP. Offline acellular tests on filtered PM are used in most conventional methods for measuring OP. These methods can cause significant delays between sample collection and analysis in addition to being time-consuming. They most likely underestimate OP since many of the reactive elements that produce it are ephemeral and decompose before analysis. To get over these limitations, a portable online device was developed that continuously samples particles and employs an ascorbic acid-based assay at physiologically appropriate settings (pH 6.8 and 37 °C). Every five minutes, it offers high-resolution measurements. The gadget enables precise OP assessments even in areas with low pollution levels, with a detection limit of about 5 $\mu g/m^3$ in urban settings and the capacity to operate independently for up to three days.

(Grange *et al.,* 2022) Oxidative potential (OP) has emerged as a key metric for assessing the biological toxicity of particulate matter (PM) in addition to traditional mass-based air quality assessment. One of the several OP tests, the ascorbic acid (AA) assay (OPAA), is widely used because it faithfully replicates the mechanism of antioxidant depletion in the human respiratory system. In a study conducted in Switzerland between June 2018 and May 2019, the OPAA, dithiothreitol (DTT), and dichlorofluorescein (DCFH) tests were assessed in five different settings: urban, suburban, and rural (Bern-Bollwerk, Payerne, Magadino-Cadenazzo, and others). The findings demonstrated that OPAA values varied over time and geography, with urban traffic sites like Bern-Bollwerk having the highest oxidative potential and rural areas like Payerne recording lower OPAA. The mean OPAA values, which ranged from 0.4 to 4.1 nmol H_2O_2 m^{-3}, varied considerably over the monitoring period based on the emission sources and weather. Importantly, OPAA levels were seasonal, increasing in the winter due to increased emissions from wood burning, particularly at the rural Magadino-Cadenazzo site. Source apportionment analysis using positive matrix factorization (PMF) models identified road traffic and wood combustion emissions as the main causes of OPAA. In particular, organic tracers like levoglucosan, mannosan, and galactosan were associated to emissions from burning wood, while metals including copper, zinc, iron, tin, antimony, manganese, and cadmium were linked to emissions from non-exhaust vehicles. Multiple linear regression modeling revealed that both metal and wood-burning tracers were the best predictors for OPAA, underscoring the interdependent effects of both sources. Importantly, the choice of a specific metal or organic tracer within each emission category was not important as long as a representative variable for the emission source was available. In order to effectively reduce OPAA and the health risks it entails; these findings emphasize the necessity of targeted mitigation initiatives that target anthropogenic emissions, particularly those caused by traffic and wood burning.

(Clemente *et al.,* 2023) Since the ascorbic acid (AA) assay (OPAA) is a popular acellular technique to evaluate the oxidative characteristics of particulate matter, the oxidative potential (OP) of PM10 has been thoroughly investigated as a gauge of its health impacts. Dithiothreitol (DTT) and OPAA activity were measured in PM10 samples taken in the summer and winter at a traffic site in southeast Spain. OPAA showed a discernible seasonal trend, with larger levels observed in the summer than in the winter, despite the fact that PM_{10} concentrations were the same in both seasons. This seasonal variation suggests that the oxidative properties of PM_{10} are influenced by different atmospheric processes and emission sources during warm and cold periods. However, the DTT assay displayed an inverted trend, with wintertime oxidative activity being higher. The varied seasonal trends of the two assays show how sensitive they are to different chemical components of PM_{10}.

Furthermore, linear correlation analysis demonstrated that OPAA was influenced by specific PM components. Additionally, the correlations varied from summer to winter, indicating that different emission sources were responsible for particle toxicity in each season. Furthermore, correlation coefficients with PM_{10} chemical species were lower when OP data were standardized by PM10 mass (nmol min^{-1} μg^{-1}) as opposed to volume-based normalization (nmol min^{-1} m^{-3}). This result implies that only some PM constituents have inherent oxidative potential and make a substantial contribution to OPAA. In order to reduce the oxidative load of airborne particles, the study emphasizes the significance of source-specific and seasonal influences on OPAA and the necessity of focused emission control measures.

3. EXPERIMENTAL PROCEDURE

3.1. Materials and chemicals

- Types of filters (e.g., Teflon membrane, pore 0.22µm, 60mm)

- Reagents (ascorbic acid, potassium phosphate buffer)
- Solvents (methanol, water)

3.2. Instrumentation and Equipment

- Low-cost air sampler
- Pump and flow rate control (rotameters, Bubble flow meter)
- SEM (Scanning Electron Microscope)
- UV-Vis Spectrophotometer
- XRF (X-ray fluorescence spectrometer)

3.3. Sample Collection

3.3.1. Location of sampling

The sampler was placed approximately 100 feet above ground level on the rooftop of the Syed Babar Ali School of Science and Engineering (SBASSE), Lahore University of Management Sciences (LUMS), to minimize local ground-level disturbances and gather ambient airborne particulate matter.;

Duration (24-hour sampling)
Flow rate (15 L/min)

3.3.2. The total number of samples collected

- A total of eight samples were collected per month from August 2024 to April 2025.
- Seasonal variations in particulate matter concentration and composition were documented by regular monitoring**.**

3.4. Description of Low-Cost $PM_{2.5}$ Sampler

A low-cost air sampler was used to gather particulate matter. The sampler consists of a baffled inlet part. Larger particles are struck and removed by the baffles when ambient air is drawn in, while tiny particles (PM2.5) travel through a central hollow pipe. The sample configuration consists of a center joint portion and two small, connected pipes. At the junction of these two pipes is a supporting net or mesh. A Teflon membrane filter is positioned strategically on this net to serve as the particulate matter collection medium. This design ensures consistent membrane support during sampling and facilitates homogenous particle deposition for the particles drawn through the device. To control and monitor the flow rate, the entire system is connected in series with a vacuum pump and a rotameter. Continuous sampling was carried out for the entire day in order to ensure sufficient particle collection for analysis.

Figure 1: Low-Cost Sampler

3.5. $PM_{2.5}$ Sampler Inlet Description

A size-selective barrier is provided by impactor wafers or baffles in the upper portion of the sampler. As ambient air enters the sampler, these wafers capture larger particles due to inertial impaction. On the other hand, tiny particles ($PM_{2.5}$ and less) go through the holes and end up on the Teflon membrane filter's surface below.

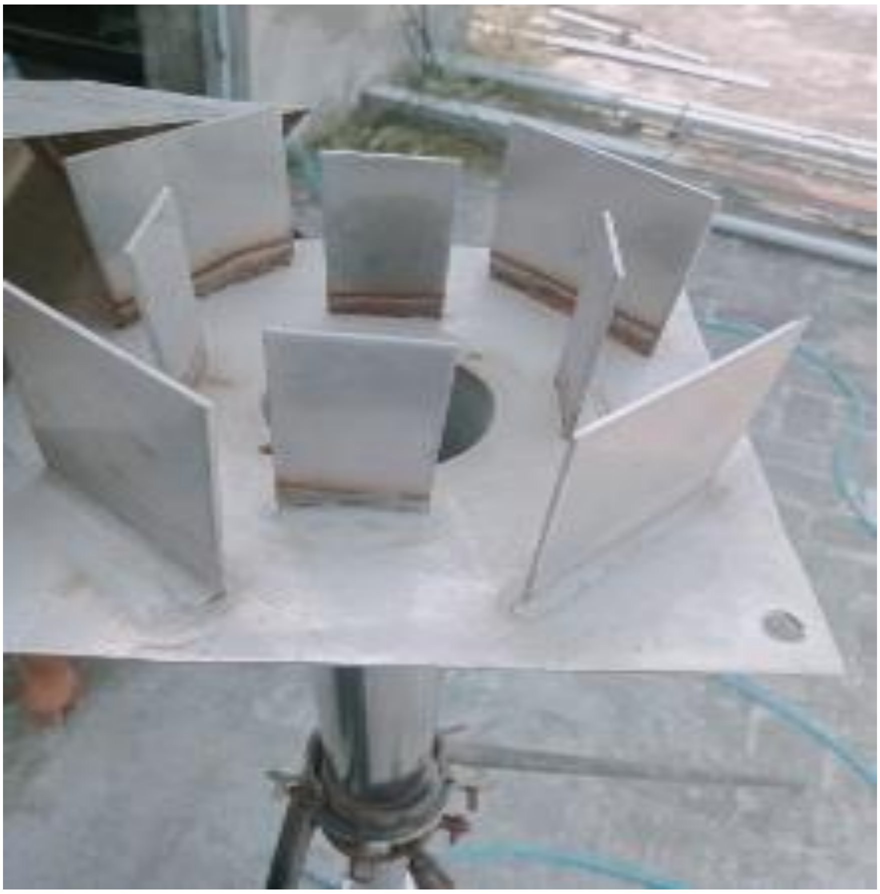

Figure 2: $PM_{2.5}$ Sampler Inlet

3.6. Sampling Procedure

- Teflon membranes were initially placed in a desiccator for a full day in order to remove any remaining moisture.
- The next day, each membrane was weighed using a microbalance and then carefully placed into the low-cost air sampler.
- The sampler was connected in series with a pump, rotameter, and bubble flow meter.
- The flow rate of air was calibrated to 15 L/min using the bubble flow meter.
- After sampling, the membranes containing particulate matter ($PM_{2.5}$) were removed and returned to the desiccator so that any moisture that had been absorbed could be removed using silica beads.
- Weighing the membranes again allowed us to determine the mass of the collected particles.

3.6.1. Each membrane was divided into four equal pieces following sampling:

- Using the water-soluble fraction, one portion was utilized for the ascorbic acid assay (AA assay).
- One portion was utilized for the methanol-soluble extract AA test. In order to remove water for further analysis, the third portion was stored.
- The fourth section was set aside for X-ray fluorescence (XRF) elemental analysis.

3.7. Experimental Procedure for Ascorbic Acid (AA) Assay

Using 30 mL of deionized (DI) water and 30 mL of methanol, a quarter of each Teflon membrane sample was sliced and extracted independently. To remove the soluble species from the particulate debris, the membranes were sonicated in both situations. In a reaction vial, 2.4 mL of each extract (water and methanol) was combined with 0.3 mL of 0.5 mM phosphate buffer (K-buffer). To remove any interference from the particles themselves, the first step was to measure the aerosol background absorbance at 265 nm and 700 nm. After that, DI water was used three times to clean the system. 0.2 mL of a 2 mM ascorbic acid solution was added to the vial in preparation for the AA activity test. The mixture was incubated at 37°C and continuously shaken at 400 rpm. Absorbance readings were taken at 10, 20, 30, 40, 50, and 60 minutes. At each interval, 100 µL of the reaction mixture was removed, diluted to 3 mL, and passed through a spectrophotometer to record the absorbance. Decrease in absorbance over time showed how much AA was consumed by the reactive species in the samples. After each run, the system was cleaned and prepared for the next sample

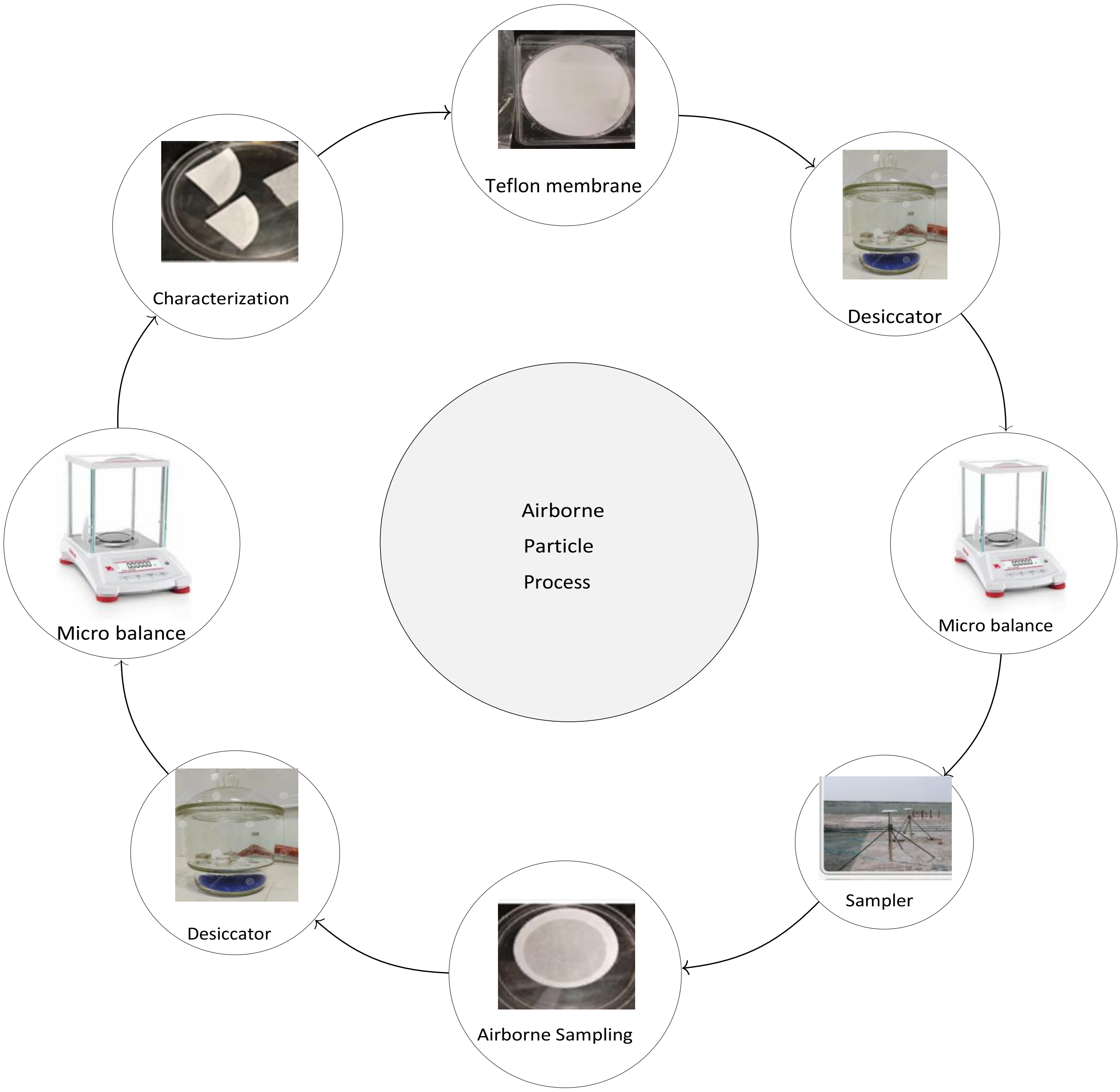

Figure 3: Schematic representation of the particle size collection methodology

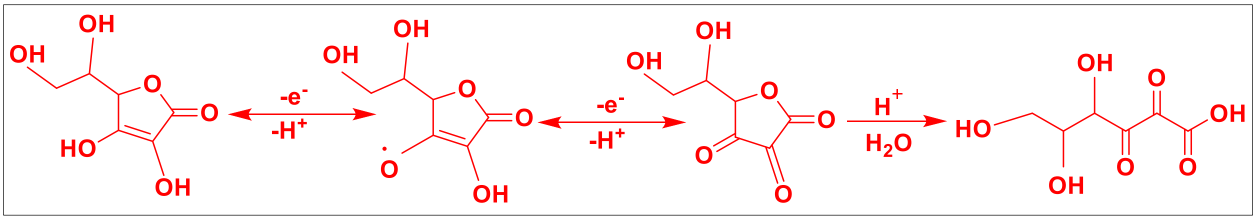

Ascorbic acid Monodehydroascorbic acid Dehydroascorbic acid 2,3-Diketogulonic acid

Ascorbic acid depletion mechanism

4. RESULTS AND DISCUSSION

4.1. Scanning Electron Microscopy (SEM)

Particulate matter ($PM_{2.5}$) was collected using a specially designed, inexpensive air sampler. To enable size-selective sampling, its entrance is baffled. The impactor wafers at the top of the device efficiently eliminated coarse particles via inertial impaction, allowing only fine particulate matter (≤2.5 μm) to pass through the central hollow channel.

On a supporting mesh downstream was a Teflon membrane filter that served as the $PM_{2.5}$ deposition medium. The complete system was connected in series with a rotameter and vacuum pump, which enabled accurate flow rate control. Continuous 24-hour sampling ensured sufficient loading for downstream SEM analysis.

subsequent SEM imaging and quantitative size distribution analysis revealed a strong dependence of particle capture efficiency on the sampling flow rate. At a flow rate of 15 L/min, particles with a diameter close to 2.5 µm dominated the distribution (Fig. 4a), indicating effective collection of upper-end fine particles. Increasing the flow rate to 20 L/min resulted in a modal diameter shift to 2.0 µm (Fig. 4b), while at 30 L/min, the peak shifted further down to 1.7 µm (Fig. 4c). These trends suggest that higher flow velocities likely reduce collection efficiency for larger fine-mode particles, either due to bounce-off effects or less efficient impaction. Lower flow conditions enhance inertial capture, favoring larger $PM_{2.5}$ retention.

SEM images revealed morphologically diverse particles, including spherical carbonaceous residues, chain-like soot aggregates, and angular mineral fragments. These morphologies indicate mixed sources such as vehicular emissions, industrial combustion, and resuspended dust. Seasonal contrasts were evident: spherical particles dominated winter samples, consistent with combustion origins, while summer filters showed increased angular and flaky particles, reflecting crustal and soil-derived sources. Thus, both sampler design and flow rate modulation played critical roles in shaping the observed particle size distributions and physical characteristics.

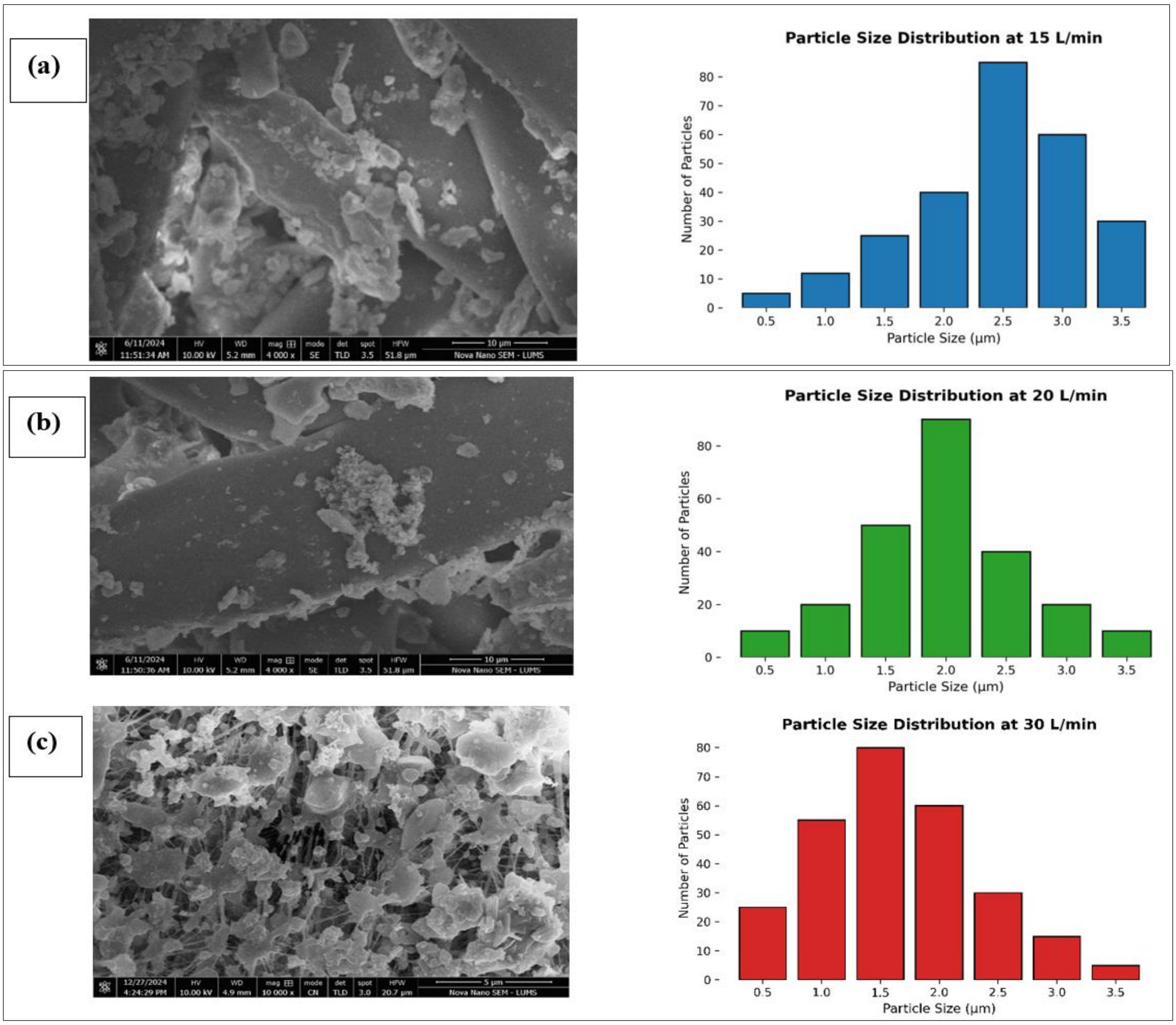

Figure 4: SEM micrographs and particle size distributions of $PM_{2.5}$ collected at different flow rates using a low-cost sampler.

(a) 15 L/min — modal diameter ≈ 2.5 µm
(b) 20 L/min — modal diameter ≈ 2.0 µm
(c) 30 L/min — modal diameter ≈ 1.7 µm

4.1. Temporal Variation of PM2.5 Concentration

To evaluate the temporal variance in fine particulate matter in the selected research area, PM2.5 concentrations were measured throughout a range of sample dates from August 2024 to April 2025. The data demonstrates a significant range in $PM_{2.5}$ levels, with values ranging from a minimum of 58.21 µg/m^3 (on March 10, 2025) to a maximum of 473.41 µg/m^3 (on November 13, 2024). The average $PM_{2.5}$ concentration during the entire sample period was far higher than the World Health Organization's (WHO) recommended 24-hour mean guideline of 25 µg/m^3, highlighting the severity of air pollution in the area.

The fall and winter months (October to January) have the greatest $PM_{2.5}$ concentrations. For instance, measurements during this period were 463.91 µg/m^3 on November 12, 434.12 µg/m^3 on October 22, and 468.52 µg/m^3 on November 6. These elevated concentrations are consistent with known seasonal pollution patterns in South Asia, where poor air quality is caused by post-harvest agricultural burning, reduced atmospheric dispersion, a lower boundary layer height, and increased use of biomass for heating.

The air quality did, however, gradually improve during the spring (March to April) season, with PM2.5 levels continuously declining below those of the preceding months. 58.21 µg/m^3 (March 10), 62.92 µg/m^3 (April 14), and 79.79 µg/m^3 (April 8) are noteworthy figures. Better atmospheric mixing, more precipitation, and enhanced photochemical reactions—all of which aid in the removal of airborne particulate matter—are probably the causes of the improvement.

Overall, a clear seasonal pattern can be seen, with the coldest seasons (autumn and winter) having the highest air pollution and the warmer spring months seeing a gradual increase in air quality. The persistently high levels of $PM_{2.5}$ during the study period raise serious concerns about the hazards to public health, especially for people who already have cardiovascular and respiratory conditions.

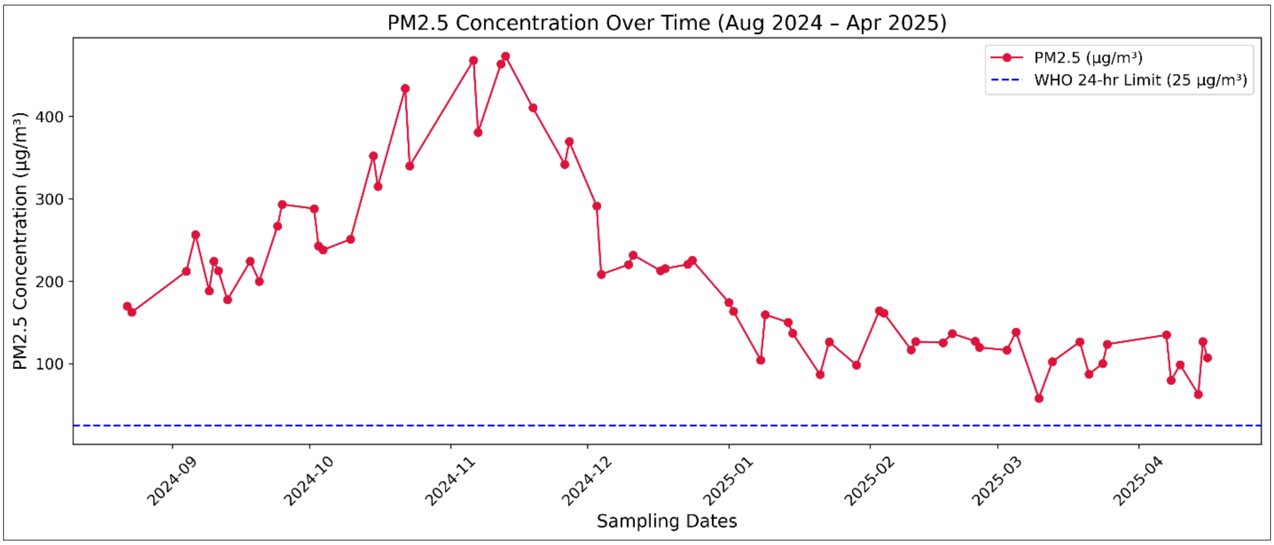

Figure 5: $PM_{2.5}$ concentration over time

Temporal Variation of Ascorbic Acid (AA) Depletion in Water-Soluble $PM_{2.5}$ Extracts

Figure 5 displays the ascorbic acid (AA) depletion rates with time in water-soluble particulate matter ($PM_{2.5}$) samples collected from August 2024 to April 2025. The depletion rate, which is expressed in nmol/(min·m^3) and indicates the oxidative potential (OP) of airborne PM_2, is evaluated using the ascorbic acid assay.

Throughout the sampling period, there was a discernible temporal variation in the rates of AA depletion. The greatest depletion rate was around 15.18 nmol/(min·m^3) in late December, after a progressive increase from initial values in August and early September that varied between ~10.6 and 12.1 nmol/(min·m^3).This seasonal trend suggests that the oxidative potential of $PM_{2.5}$ increased during the winter months due to increased emissions from combustion-related activities (such as burning biomass, traffic, and heating) and atmospheric conditions that favor pollutant accumulation (such as temperature inversions and low boundary layer height).

AA depletion levels decreased in January and February after the winter peak, and then they were relatively stable but somewhat lower in the early spring (March–April 2025). These results are consistent with seasonal changes in PM composition and source profiles, which are known to influence the oxidative potential of particulate matter.

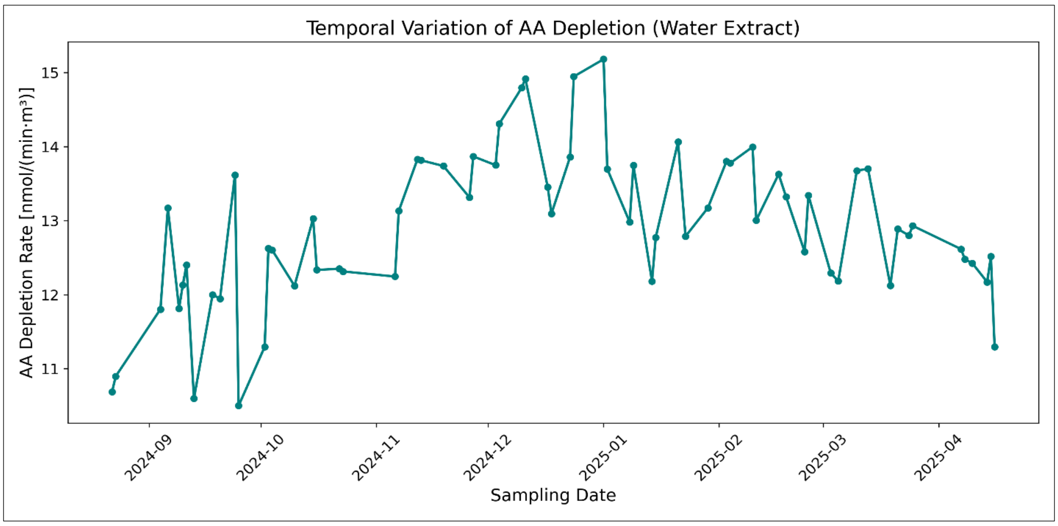

Figure 6:Seasonal variation of AA depletion rates in water-soluble $PM_{2.5}$ extracts from August 2024 to April 2025, showing peak oxidative potential in winter.

4.1. Temporal Variation in Methanol-Soluble Oxidative Potential of $PM_{2.5}$

The ascorbic acid (AA) depletion rate trend for $PM_{2.5}$ samples extracted with methanol from August 2024 to April 2025 is shown in Figure X. The oxidative potential (OP) of particulate matter is represented by the AA depletion rate, which is measured in nmol/(min·m³) and indicates the ability of ambient aerosols to produce reactive oxygen species (ROS) through redox-active components.

Throughout the study period, the depletion data showed temporal variability, with a discernible rise during the winter months (December to February), when AA depletion rates often above 15 nmol/(min·m³). This seasonal rise in OP is in line with earlier research and could be brought on by lower atmospheric mixing heights that encourage pollutant buildup, greater vehicle emissions from temperature inversions, and increased emissions from combustion (such as burning biomass for warmth).

Conversely, lower depletion rates were generally observed in late summer and early fall (August–September), indicating that periods of enhanced photochemical activity and improved dispersion conditions led to reduced oxidative stress in the atmosphere.

The absence of grid lines in the picture enhances clarity and visual focus on the trends, even though the crimson-colored line depicts variance across time. These findings show how oxidative potential in urban atmospheres is dynamic and how important it is to consider seasonal variations when assessing aerosol toxicity.

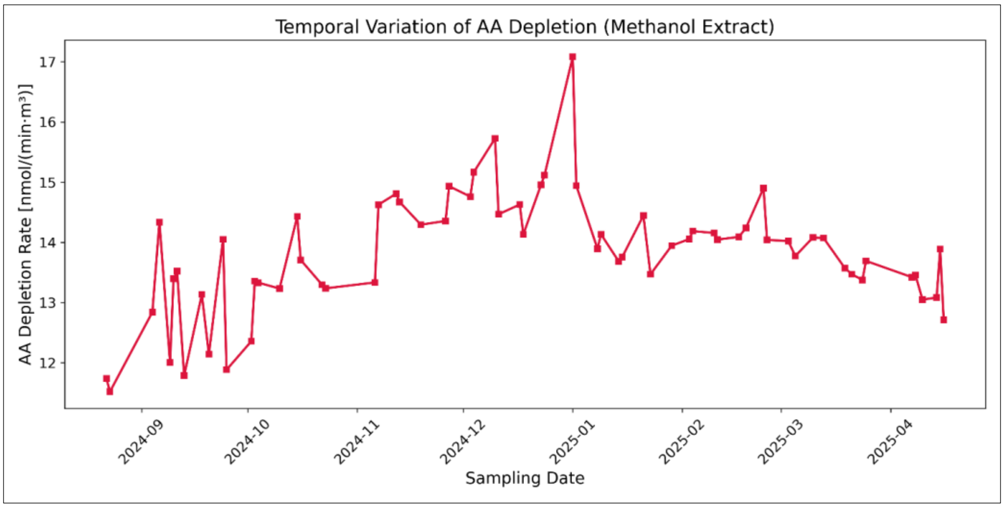

Figure 7: Time-series plot of ascorbic acid (AA) depletion rates for methanol-extracted $PM_{2.5}$ samples. Data spans from August 2024 to April 2025. The depletion rate, an indicator of oxidative potential, reveals seasonal patterns with peaks in colder months. Higher oxidative activity in winter may be attributed to increased biomass burning, vehicular emissions, and atmospheric stagnation

4.1. Correlation Analysis of PM2.5 with Meteorological Parameters

To understand how climatic conditions affect PM2.5 concentrations, basic linear regression and Pearson correlation tests were performed between PM2.5 levels and three key parameters: temperature, relative humidity (RH), and wind speed. The dataset covered 60 sampling days between August 2024 and April 2025.

Overall, there was minimal correlation between PM2.5 concentrations and the meteorological factors. The Pearson correlation between temperature and PM2.5 was r = -0.008, indicating that there was no clear linear relationship between the two variables. Similarly, there was a correlation between wind speed and r = -0.234 and r = 0.106 with relative humidity. These findings demonstrate that while temperature and humidity had minimal relationship with PM2.5, wind speed showed a slight negative association with PM2.5, indicating that higher winds may slightly reduce PM2.5 concentrations.

Basic linear regression analyses were then used to validate these findings. The coefficient of determination (R2) for temperature and PM2.5 was 0.00007, for RH and PM2.5 it was 0.011, and for wind speed and PM2.5 it was 0.055. These poor R2 values suggest that none of the meteorological factors by themselves were able to adequately explain the variation in PM2.5 concentrations over the course of the study.

Despite the limited statistical connections, this investigation must be included. It highlights the complexity of air pollution dynamics and suggests that other factors, such emission sources, atmospheric stability, or long-distance pollutant transport, might have a bigger impact on PM2.5 levels. These findings are consistent with comparable studies conducted in metropolitan environments, where meteorology alone is often unable to account for the high degree of variability in particulate matter concentrations.

Overall, the analysis supports the idea that future research should examine additional factors as emission inventories, topographical effects, or the chemical composition of PM2.5 and highlights the need of multifactorial methodologies in air quality research.

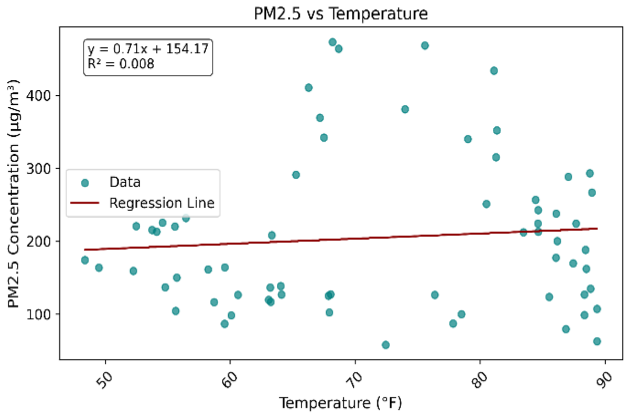

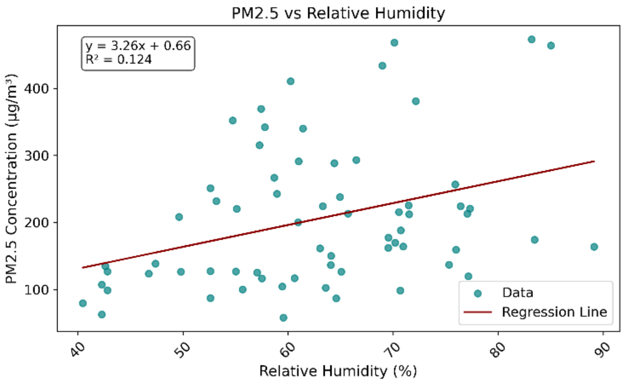

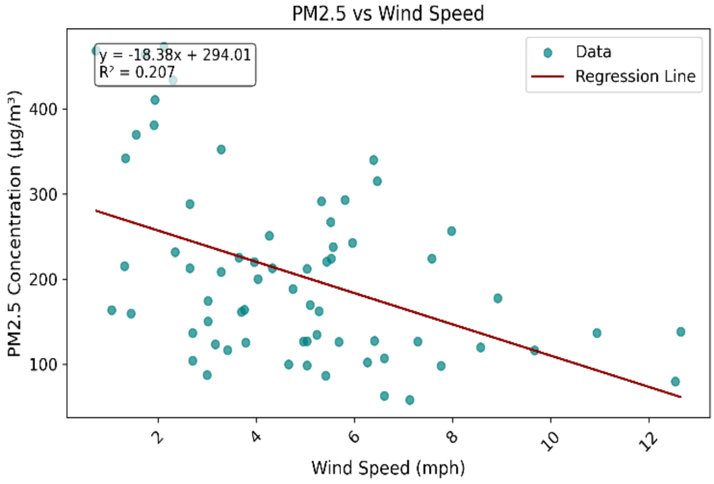

Figure 8: Scatter plots showing the relationships between $PM_{2.5}$ concentration (µg/m³) and meteorological variables: temperature (°F), relative humidity (%), and wind speed (mph). Weak correlations suggest that no single weather parameter alone strongly influences $PM_{2.5}$ levels, highlighting the complex interactions between meteorology and particulate pollution.

4.1. Relationship Between PM2.5 and Ascorbic Acid Depletion Rate

The oxidative potential of airborne fine particulate matter was evaluated using the rate of ascorbic acid (AA) depletion in the water-soluble component of PM2.5 as a redox activity indicator. This experiment illustrates the possibility of particle-induced oxidative stress, which has an impact on human respiratory health.

The oxidative potential of airborne fine particulate matter was evaluated using the rate of ascorbic acid (AA) depletion in the water-soluble component of PM2.5 as a redox activity indicator. This experiment illustrates the possibility of particle-induced oxidative stress, which has an impact on human respiratory health.

AA Depletion Rate=0.00045×$PM_{2.5}$+12.88

As seen by the incredibly weak correlation (r = 0.033, p = 0.7868) and R2 value of 0.005, there was no statistically significant linear relationship between PM2.5 and AA depletion rate. This suggests that particle mass concentration alone is insufficient to predict oxidative potential.

$$AA\ Depletion_{(H_2O)} = 0.00045 \times PM_{2.5} + 12.88$$

This result is consistent with previous research showing that chemical composition, specifically the presence of redox-active species such as quinones and transition metals (Fe, Cu, and Mn), has a stronger effect on oxidative activity than does the mass concentration of PM2.5 overall. In this study, AA depletion was higher in samples with lower PM2.5 masses, suggesting that certain particles are more dangerous per unit mass.

The fact that a seasonal categorization of the data (based on the sample date) did not reveal any distinct grouping or patterns further supports the significance of emission source categories such as transportation, biomass burning, or industrial operations rather than just weather.

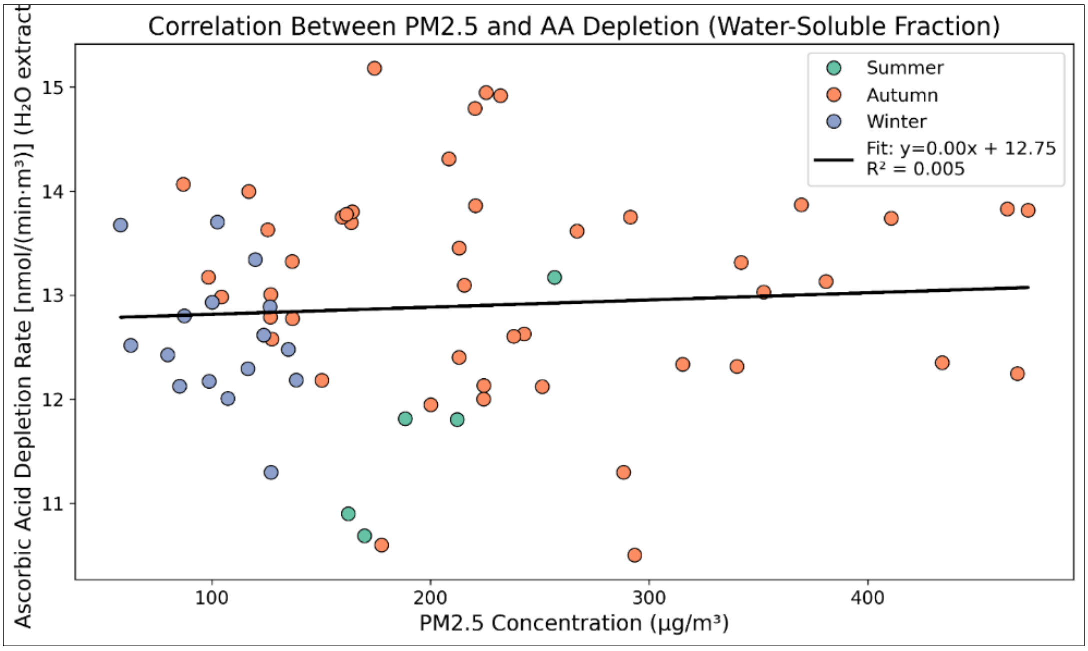

Figure 9: Scatter plot showing the relationship between PM2.5 concentration (µg/m³) and the ascorbic acid (AA) depletion rate [nmol/(min·m³)]. Data points are color-coded by season. A linear regression line is shown with the equation and R² value. The weak correlation suggests that oxidative potential is not directly proportional to particle mass but rather to compositional factors

Correlation Between $PM_{2.5}$ Mass Concentration and Oxidative Potential Measured by AA Depletion in Methanol Extracts

The study discovered a very modest positive correlation (coefficient of determination R2 = 0.015) between the rate of AA depletion and the mass concentration of PM_2. This suggests that only around 1.5% of the variation in oxidative potential (as measured by AA depletion in methanol) can be explained by $PM_{2.5}$ concentration alone (Figure X). The slightly positive slope of the regression line showed a minor increase in AA depletion with increasing $PM_{2.5}$ levels.

$$AA\ Depletion_{(CH_3OH)} = 0.0039 \times PM_{2.5} + 12.89$$

The low R² indicates that $PM_{2.5}$ mass is not a reliable indicator of oxidative activity in methanol extracts. This study supports the understanding that oxidative potential is dependent on chemical composition rather than just particle bulk. Redox-active substances, such as organic compounds (like quinones and PAHs) and transition metals (including Cu, Fe, and Mn), may significantly affect AA depletion even at lower PM concentrations.

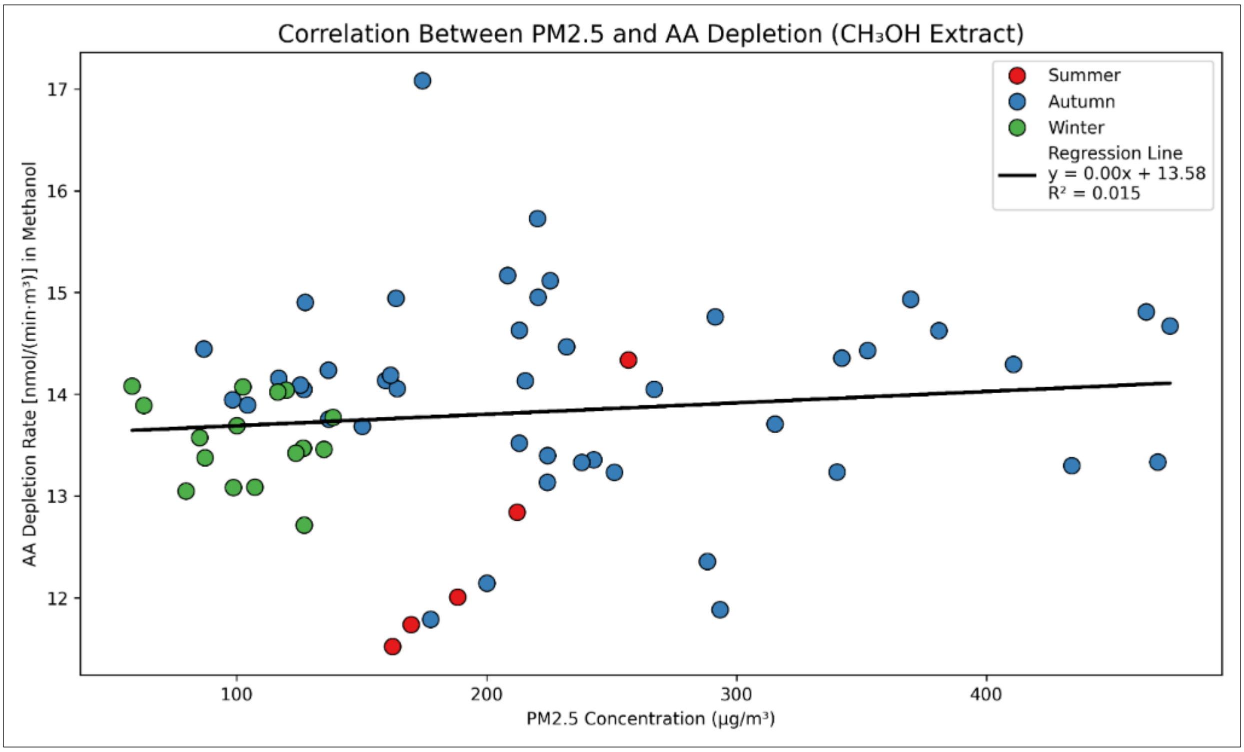

Figure 10: Scatter plot depicting the relationship between $PM_{2.5}$ concentration (µg/m³) and the AA depletion rate [nmol/(min·m³)] measured in methanol extracts. Data points are color-coded by season. The solid black line represents the linear regression fit with an R² value indicating the strength of the correlation

Table 1: Regression Analysis of AA Depletion Rates with $PM_{2.5}$ Concentration

Extract Type	**Regression Equation**	**R²**	**p-value**
Water (H_2O)	AA = 0.00045 × $PM_{2.5}$ + 12.88	0.005	0.7868
Methanol (CH_3OH)	AA = 0.0039 × $PM_{2.5}$ + 12.89	0.015	Not significant

Linear regression equations, coefficients of determination (R^2), and p-values show the relationship between $PM_{2.5}$ mass concentration and oxidative potential (measured by ascorbic acid (AA) depletion) in both water and methanol extracts. The low R^2 values demonstrate that PM_2 mass by itself is not a reliable indicator of oxidative activity.

Explanation (for Monthly and Seasonal Trends)

The monthly and seasonal variation of PM_2 concentrations was analyzed in order to assess temporal trends in particulate matter levels. As seen in Figure X, $PM_{2.5}$ concentrations clearly vary with the seasons, with higher levels observed throughout the winter (December to February, for example). This tendency is most likely caused by temperature inversions, stagnant air conditions that hinder the dispersal of pollutants, and increased fossil fuel combustion for heating.

Conversely, concentrations tend to be lower during the summer, which could be due to a combination of factors such as greater air mixing, rainfall-induced wet deposition, and a decline in emissions from human activity. The violin plots provide a comprehensive knowledge of the density and dispersion of the data and highlight months with higher fluctuation in pollutant levels. The seasonal aggregate further supports the finding that winter has the highest median $PM_{2.5}$ concentrations when compared to other seasons.

These results highlight the need for targeted mitigation strategies during periods of high pollution and show how seasonal weather patterns and human activity impact ambient air quality.

Comparison of Ascorbic Acid Depletion Rates in Water and Methanol Extracts of $PM_{2.5}$ Samples

This graph uses the ascorbic acid depletion experiment to assess the oxidative potential of PM2.5 fractions that are soluble in methanol and water. Ascorbic acid (AA), a substitute antioxidant, assesses the ability of particulate matter to generate reactive oxygen species (ROS).

Four samples (Samples 1 through 4) were analyzed. For both methanol and water extracts, the rate of AA depletion was measured. The results consistently show that methanol extracts deplete more quickly than their water counterparts. Specifically, Sample 3 showed the highest depletion rate in methanol 14.2 ± 0.7 [nmol/(min·m³)] and the lowest in water [11.9 ± 0.6 nmol/(min·m³)].

This suggests that the organic-soluble species in $PM_{2.5}$ that are extracted by methanol have a higher potential to induce oxidative stress than the water-soluble portion. These findings are important for evaluating environmental health since they demonstrate the presence of dangerous, redox-active organic compounds in ambient air particles.

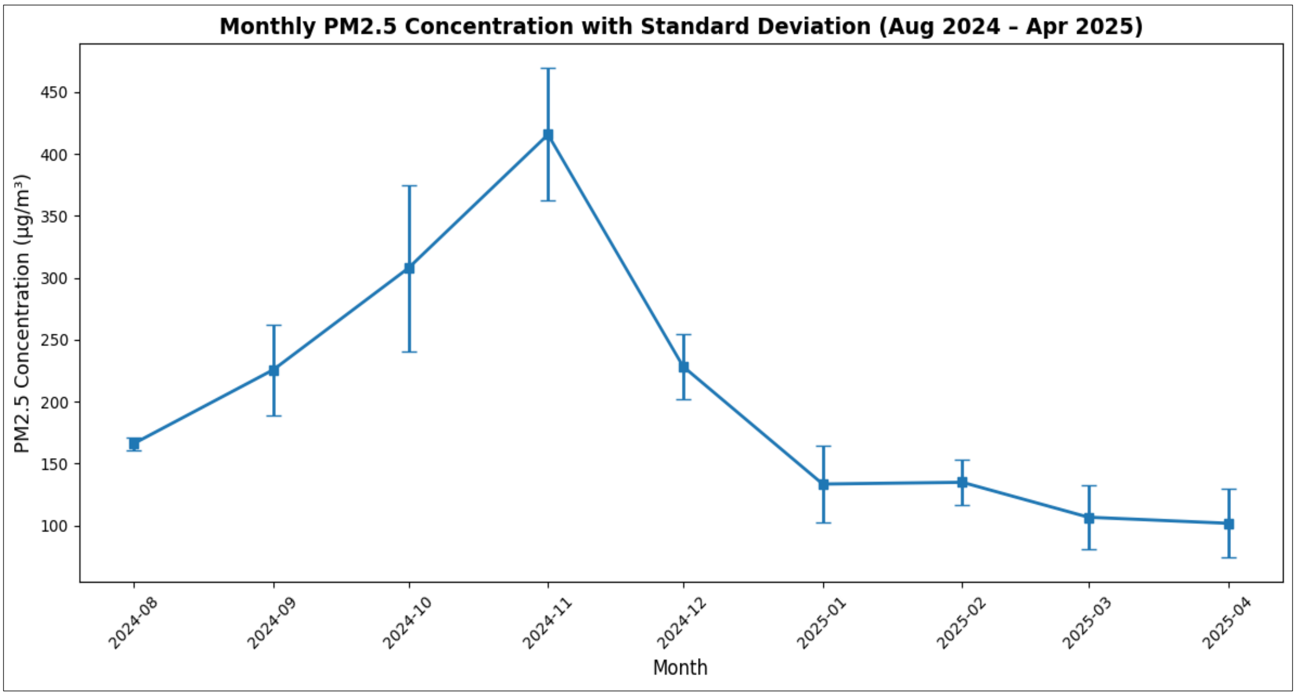

Figure 11: The graph illustrates the monthly average PM2.5 concentration (µg/m³) measured from August 2024 to April 2025. Error bars denote ± one standard deviation, based on all sampling dates within each month

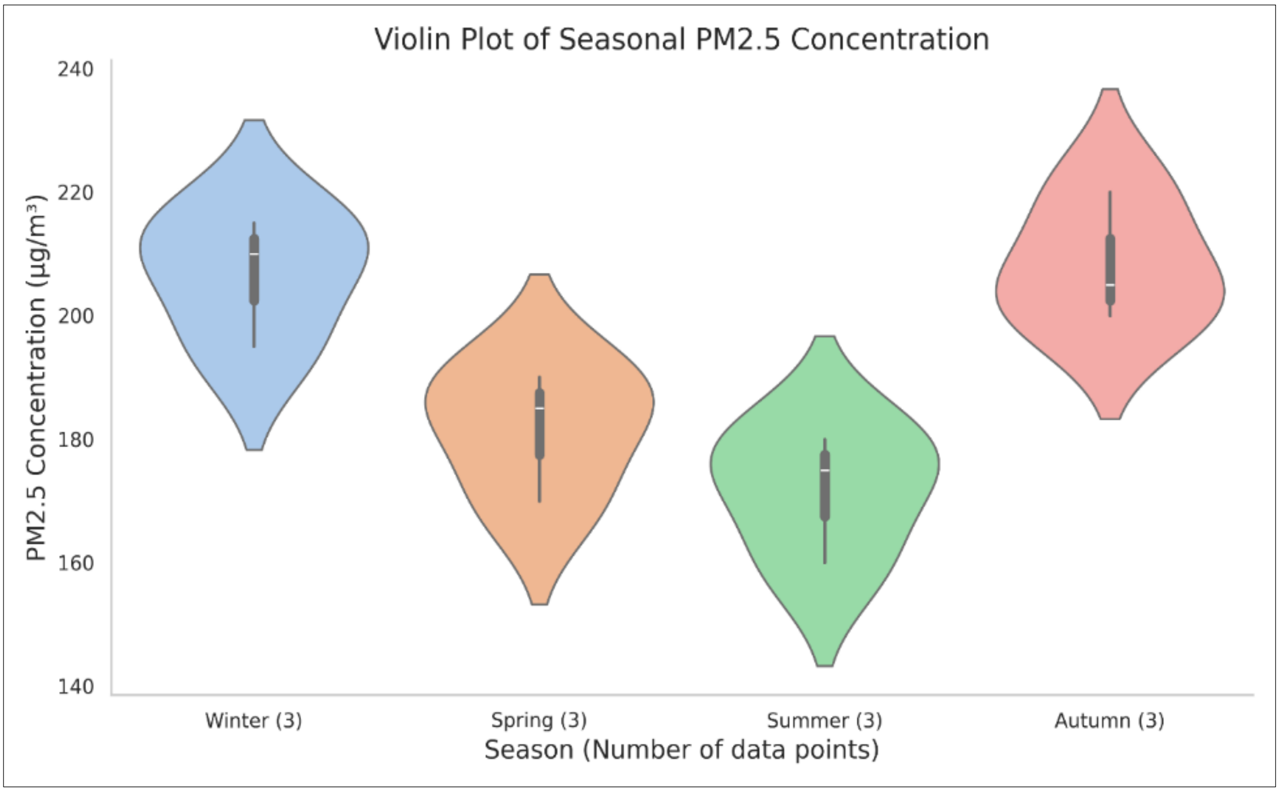

Figure 12: Seasonal variation of $PM_{2.5}$ concentrations represented using a violin plot. The plot displays the distribution, central

tendency (median), and variability (interquartile range) for each season. The number of recorded data points per season is indicated in parentheses

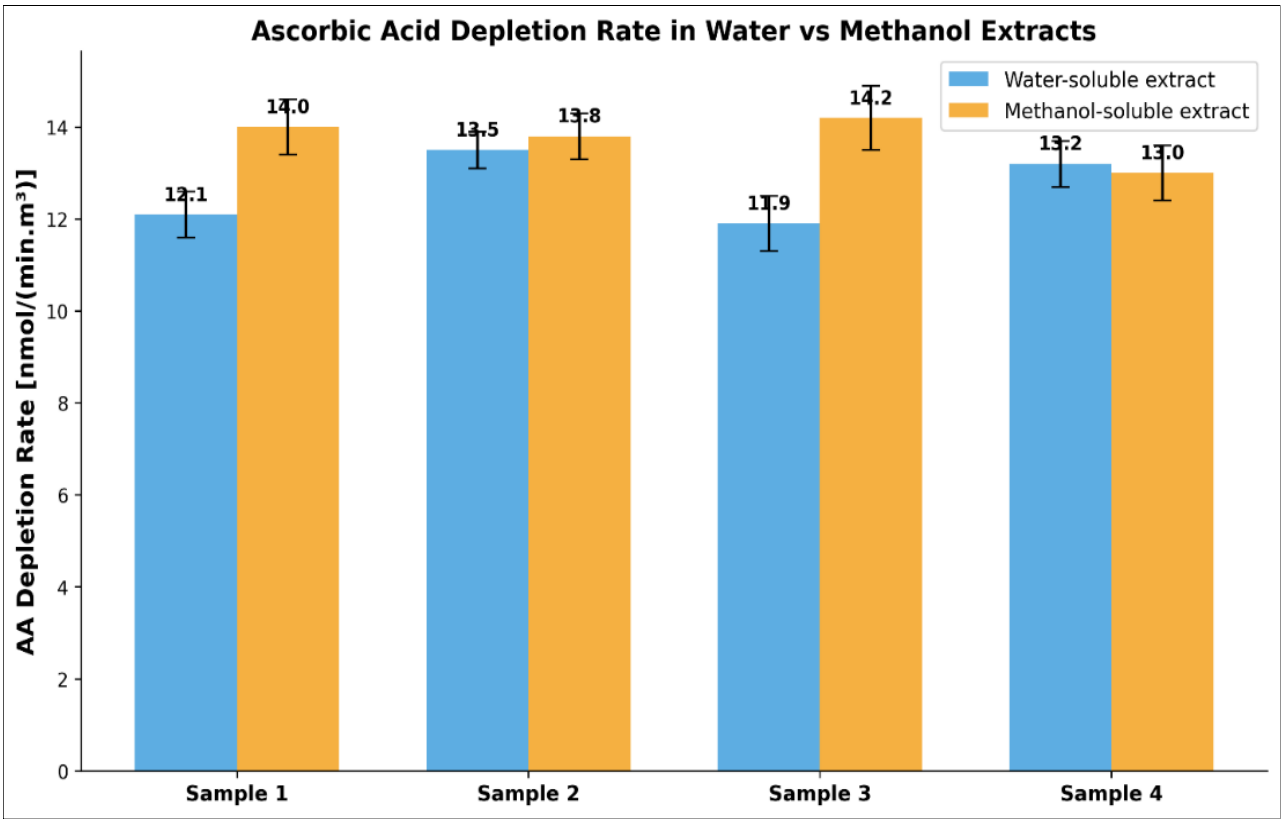

Figure 13: shows a bar graph showing the rates of ascorbic acid (AA) depletion in particulate matter ($PM_{2.5}$) samples extracted using methanol and water. The unit of measurement for the rate of depletion is nanomoles per minute per cubic meter (nmol/(min·m³)). Methanol extracts frequently exhibit higher rates of depletion than water extracts, indicating a greater capability for oxidation. Error bars represent the standard deviation obtained from replicate measurements

Association of $PM_{2.5}$ with Metal Content and Its Implication for Oxidative Potential

To ascertain the potential redox activity of PM_2, we analyzed the concentrations of redox-active elements such as Fe, Cu, and Zn. These metals are known to contribute significantly to the development of oxidative stress through catalytic redox cycling. The results indicate that these metal concentrations and $PM_{2.5}$ mass are positively correlated (Figure X). According to its crustal and anthropogenic sources, iron had the greatest range of concentrations among the metals. Although in varying amounts, Cu and Zn, which are commonly associated with emissions from automobiles and industry, also increased with PM_2. These trends support studies demonstrating that transition metals, not PM mass alone, significantly influence particle oxidative potential(Charrier & Anastasio, 2012).

These results demonstrate how important it is to include chemical speciation when evaluating the health risks associated with particulate matter. Importantly, elevated levels of Fe and Cu may raise the risk of oxidative stress during inhalation by increasing the generation of ROS through Fenton-like processes, even at moderate $PM_{2.5}$ concentrations.

Regression of Selected Metals (Mn, Pb, As) vs. $PM_{2.5}$ Concentration

A statistical investigation was conducted into the correlation between $PM_{2.5}$ concentrations and specific metal elements (Mn, Pb, and As). Using linear regression analysis, various correlation levels were discovered. Manganese and lead showed moderate to mild negative associations (R2 = 0.3752 and 0.2096, respectively) with $PM_{2.5}$, while arsenic showed a moderately positive correlation (R2 = 0.4138).The respective regression equations were:

$$\mathbf{Mn = -298.16 \times PM_{2.5} + 71,081.05}$$
$$\mathbf{Pb = -174.63 \times PM_{2.5} + 46,977.50}$$
$$\mathbf{As = +1045.46 \times PM_{2.5} - 194,962.45}$$

These results suggest that while $PM_{2.5}$ concentration contributes somewhat to predicting metal levels, especially in the case of arsenic, it is not a strong standalone predictor for all metals studied.

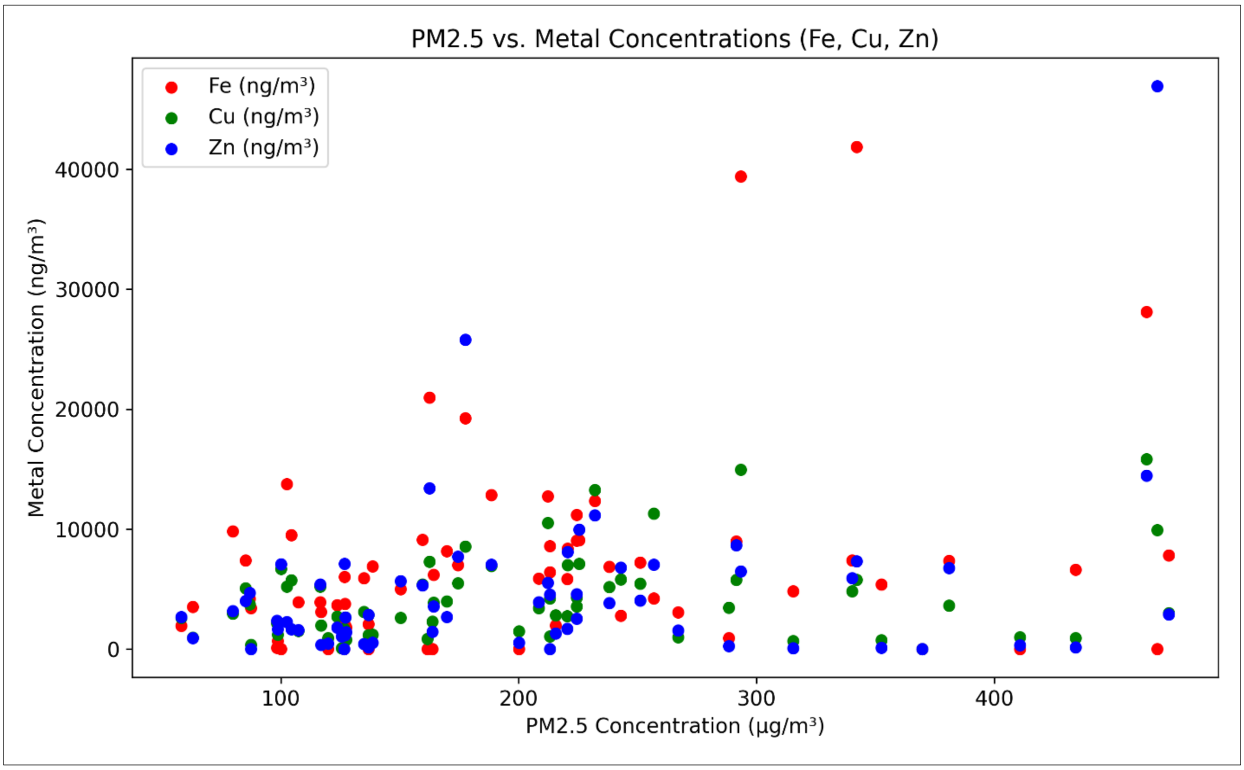

Figure 14: Scatter Plot Showing the Relationship Between $PM_{2.5}$ Concentration and Selected Metal Concentrations (Fe, Cu, Zn)

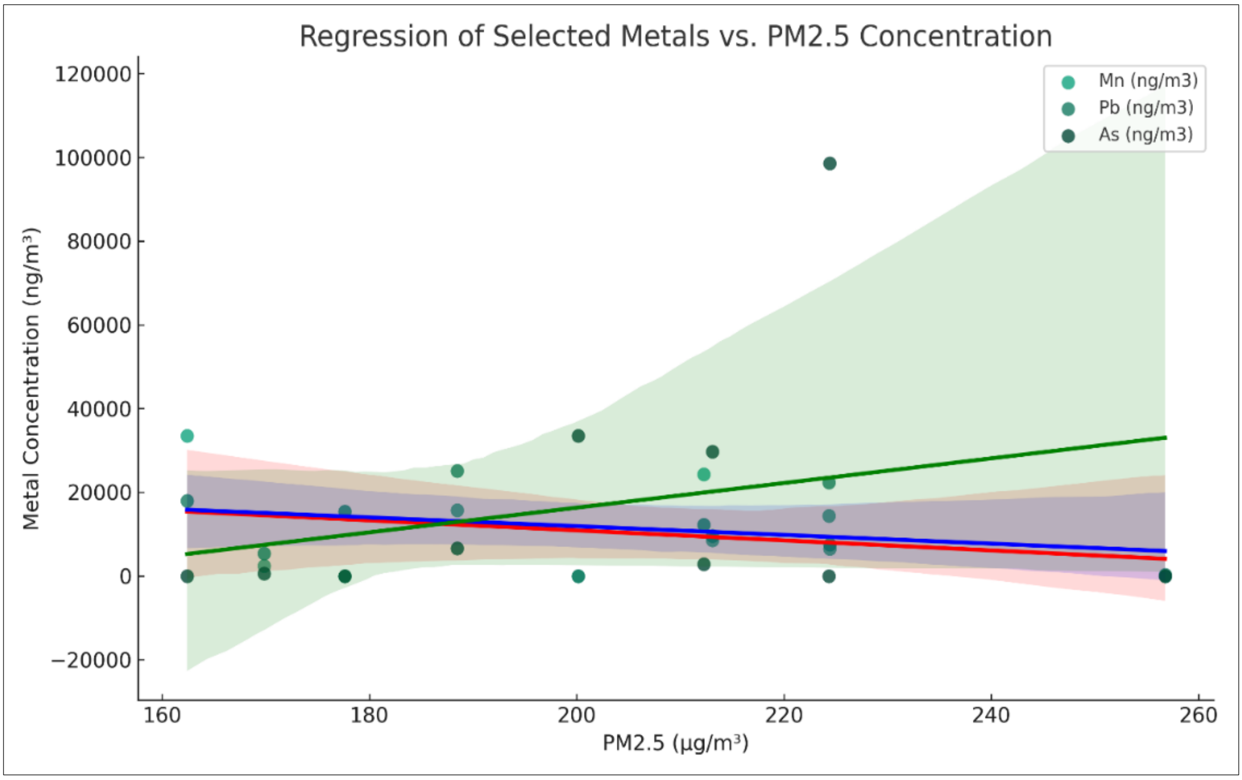

Figure 15 : Scatter plots and linear regression lines for the relationship between $PM_{2.5}$ concentration (µg/m³) and concentrations (ng/m³) of Mn, Pb, and As. The relationships between Mn and As were moderate, while Pb showed a less clear pattern. These results imply that metal concentrations, which are not solely regulated by $PM_{2.5}$ mass, are likely to be influenced by source variability and metal-specific emission patterns

Table 2: Linear regression equations and coefficients of determination (R^2) showing the relationship between $PM_{2.5}$ mass concentration (μg/m³) and the concentrations (ng/m³) of selected metals

Metal	Regression Equation	R²	Trend
Mn	$Mn = -298.16 \times PM_{2.5} + 71{,}081.05$	0.3752	Moderate negative
Pb	$Pb = -174.63 \times PM_{2.5} + 46{,}977.50$	0.2096	Weak negative
As	$As = +1045.46 \times PM_{2.5} - 194{,}962.45$	0.4138	Moderate positive

The minor correlation between arsenic and PM_2 mass may be caused by specific combustion sources, such as burning coal or biomass, which release both fine particles and arsenic compounds. Conversely, lead and manganese displayed weaker relationships, which might be due to differences in particle size fractions and distinct emission sources.

These results are in line with previous research by Verma *et al.,,* (2014), who found that metal speciation and solubility have a greater impact on $PM_{2.5}$ oxidative potential and toxicity than total particle mass. (Charrier & Anastasio, 2012) further highlighted the part soluble transition metals play in redox activity, which might not scale linearly with the concentration of PM_2.

The weak-to-moderate R^2 values observed here indicate that more seasonal or diurnal research and source apportionment analysis are needed to fully understand metal–PM interactions and their health effects.

5. CONCLUSION

This study provides a comprehensive physicochemical and toxicological characterization of ambient $PM_{2.5}$ collected using a low-cost, size-selective air sampler. Through SEM imaging and size distribution analysis, we demonstrate that both particle morphology and aerodynamic diameter are strongly modulated by flow rate, with lower sampling velocities favoring the retention of larger fine particles. The morphological heterogeneity—ranging from soot-like aggregates to angular crustal fragments—reflects a dynamic mix of anthropogenic and natural sources whose contributions shift seasonally.

Our temporal analysis of $PM_{2.5}$ concentrations from August 2024 to April 2025 reveals pronounced seasonal variation, with pollution levels peaking in late autumn and winter due to atmospheric stagnation, biomass burning, and low boundary layer height. Oxidative potential, quantified through ascorbic acid depletion assays, followed similar seasonal patterns, with higher AA depletion rates during winter months, particularly in methanol-soluble fractions, indicating a higher abundance of redox-active organic compounds during periods of combustion-intensive activity.

Interestingly, no significant correlation was found between $PM_{2.5}$ mass and oxidative potential, reinforcing the notion that chemical composition, rather than mass concentration, is the key driver of toxicity. While transition metals such as Fe, Cu, and Zn were positively associated with $PM_{2.5}$ levels, regression analysis with individual metals such as Mn, Pb, and As revealed source-dependent and element-specific trends, underscoring the importance of chemical speciation in health risk assessments.

Overall, these findings highlight the multifactorial nature of $PM_{2.5}$ toxicity, shaped by source contributions, seasonal meteorology, and complex interactions between particle-bound organics and metals. This underscores the critical need to move beyond mass-based regulations and toward composition-aware air quality management strategies, especially in rapidly urbanizing regions vulnerable to episodic pollution events.

REFERENCES

- Abdul-Wahab, S. A. (2004). Source characterization of atmospheric heavy metals in industrial/residential areas: a case study in Oman. *Journal of the Air & Waste Management Association*, *54*(4), 425-431.
- Alghamdi, M. A. (2016). Characteristics and risk assessment of heavy metals in airborne PM 10 from a Residential Area of Northern Jeddah City, Saudi Arabia. *Polish Journal of Environmental Studies*, *25*(3).
- Anderson, J. O., Thundiyil, J. G., & Stolbach, A. (2012). Clearing the air: a review of the effects of particulate matter air pollution on human health. *Journal of medical toxicology*, *8*, 166-175.
- Blades, M. (2022). Letters to the Editor: H-Classic Papers in Atomic Spectroscopy.
- Brown, R. A., Stevanovic, S., Bottle, S., & Ristovski, Z. D. (2019). An instrument for the rapid quantification of PM-bound ROS: the Particle Into Nitroxide Quencher (PINQ). *Atmospheric Measurement Techniques*, *12*(4), 2387-2401.
- Campbell, S. J., Utinger, B., Barth, A., Paulson, S. E., & Kalberer, M. (2023). Iron and copper alter the oxidative potential of secondary organic aerosol: insights from online measurements and model development. *Environmental science & technology*, *57*(36), 13546-13558.
- Charrier, J. G., & Anastasio, C. (2012). On dithiothreitol (DTT) as a measure of oxidative potential for ambient particles: evidence for the importance of soluble transition metals. *Atmospheric chemistry and physics (Print)*, *12*(5), 11317.
- Cheema, A. M., Majeed, M. F., & Iftikhar, A. (2024). AIR POLLUTION MANAGEMENT: HARMONIZING ENVIRONMENTAL AND ISLAMIC VIEWPOINT. *Jahan-e-Tahqeeq*, *7*(1), 1357-1372.

- Chen, Y., & Liu, X. (2023). Determinants of Beijing residents' intentions to take protective behaviors against smog: an application of the health belief model. *Health Communication*, *38*(3), 447-459.
- Choi, E., Yi, S.-M., Lee, Y. S., Jo, H., Baek, S.-O., & Heo, J.-B. (2022). Sources of airborne particulate matter-bound metals and spatial-seasonal variability of health risk potentials in four large cities, South Korea. *Environmental Science and Pollution Research*, *29*(19), 28359-28374.
- Clemente, Á., Gil-Moltó, J., Yubero, E., Juárez, N., Nicolás, J., Crespo, J., & Galindo, N. (2023). Sensitivity of PM10 oxidative potential to aerosol chemical composition at a Mediterranean urban site: ascorbic acid versus dithiothreitol measurements. *Air Quality, Atmosphere & Health*, *16*(6), 1165-1172.
- Daellenbach, K. R., Uzu, G., Jiang, J., Cassagnes, L.-E., Leni, Z., Vlachou, A., Stefenelli, G., Canonaco, F., Weber, S., & Segers, A. (2020). Sources of particulate-matter air pollution and its oxidative potential in Europe. *Nature*, *587*(7834), 414-419.
- Dedoussi, I. C., Eastham, S. D., Monier, E., & Barrett, S. R. (2020). Premature mortality related to United States cross-state air pollution. *Nature*, *578*(7794), 261-265.
- Dubey, S., Vijay, P., Raparthi, N., & Phuleria, H. C. (2024). Investigating PM 2.5 Oxidative Potential and Its Association with Chemical Constituents Measured outside of Urban Residences in Three Metropolitan Cities of India. *Journal of Health and Pollution*, *12*(1-4), 017004.
- Esworthy, R. (2013). Air quality: EPA's 2013 changes to the particulate matter (PM) standard.
- Grange, S. K., Uzu, G., Weber, S., Jaffrezo, J.-L., & Hueglin, C. (2022). Linking Switzerland's PM 10 and PM 2.5 oxidative potential (OP) with emission sources. *Atmospheric Chemistry and Physics*, *22*(10), 7029-7050.
- Grantz, D., Garner, J., & Johnson, D. (2003). Ecological effects of particulate matter. *Environment international*, *29*(2-3), 213-239.
- Grover, B. D., Carter, C. B., Kleinman, M. A., Richards, J. S., Eatough, N. L., Eatough, D. J., Dasgupta, P. K., Al-Horr, R., & Ullah, S. R. (2006). Monitoring and source apportionment of fine particulate matter at Lindon, Utah. *Aerosol science and technology*, *40*(10), 941-951.
- Guillerm, N., & Cesari, G. (2015). Fighting ambient air pollution and its impact on health: from human rights to the right to a clean environment. *The international journal of tuberculosis and lung disease*, *19*(8), 887-897.
- Harper, S. L., Walling, J. F., Holland, D. M., & Pranger, L. J. (1983). Simplex optimization of multielement ultrasonic extraction of atmospheric particulates. *Analytical Chemistry*, *55*(9), 1553-1557.
- Harrison, R. M., & Yin, J. (2000). Particulate matter in the atmosphere: which particle properties are important for its effects on health? *Science of the total environment*, *249*(1-3), 85-101.
- Hoffmann, B., Boogaard, H., de Nazelle, A., Andersen, Z. J., Abramson, M., Brauer, M., Brunekreef, B., Forastiere, F., Huang, W., & Kan, H. (2021). WHO air quality guidelines 2021–aiming for healthier air for all: a joint statement by medical, public health, scientific societies and patient representative organisations. *International journal of public health*, *66*, 1604465.
- Huang, R.-J., Zhang, Y., Bozzetti, C., Ho, K.-F., Cao, J.-J., Han, Y., Daellenbach, K. R., Slowik, J. G., Platt, S. M., & Canonaco, F. (2014). High secondary aerosol contribution to particulate pollution during haze events in China. *Nature*, *514*(7521), 218-222.
- Jameson, L. E., Conrow, K. D., Pinkhasova, D. V., Boulanger, H. L., Ha, H., Jourabchian, N., Johnson, S. A., Simeone, M. P., Afia, I. A., & Cahill, T. M. (2022). Comparison of state-level regulations for cannabis contaminants and implications for public health. *Environmental Health Perspectives*, *130*(9), 097001.
- Jellal, I., Vergnes, H., & Caussat, B. (2024). Fluidized Bed Chemical Vapor Deposition of Copper on Micronic Alumina Powders. *Chemical Engineering & Technology*, *47*(12), e202400253.
- Jeong, C.-H., McGuire, M., Godri, K., Slowik, J., Rehbein, P., & Evans, G. (2011). Quantification of aerosol chemical composition using continuous single particle measurements. *Atmospheric Chemistry and Physics*, *11*(14), 7027-7044.
- Kero, I. T., Blom, A., & Jørgensen, R. B. (2021). Particle size distributions of airborne particulate matter in a ferrosilicon smelter. Proceedings of the 16th International Ferro-Alloys Congress (INFACON XVI),
- Kero, I. T., & Jørgensen, R. B. (2016). Comparison of three real-time measurement methods for airborne ultrafine particles in the silicon alloy industry. *International journal of environmental research and public health*, *13*(9), 871.
- Khodeir, M., Shamy, M., Alghamdi, M., Zhong, M., Sun, H., Costa, M., Chen, L.-C., & Maciejczyk, P. (2012). Source apportionment and elemental composition of PM2. 5 and PM10 in Jeddah City, Saudi Arabia. *Atmospheric pollution research*, *3*(3), 331-340.
- Lakey, P. S., Berkemeier, T., Tong, H., Arangio, A. M., Lucas, K., Pöschl, U., & Shiraiwa, M. (2016). Chemical exposure-response relationship between air pollutants and reactive oxygen species in the human respiratory tract. *Scientific reports*, *6*(1), 32916.
- Lee, B.-K., & Hieu, N. T. (2011). Seasonal variation and sources of heavy metals in atmospheric aerosols in a residential area of Ulsan, Korea. *Aerosol and Air Quality Resarch*, *11*(6), 679-688.
- Lelieveld, S., Wilson, J., Dovrou, E., Mishra, A., Lakey, P. S., Shiraiwa, M., Pöschl, U., & Berkemeier, T. (2021). Hydroxyl radical production by air pollutants in epithelial lining fluid governed by interconversion and scavenging of reactive oxygen species. *Environmental science & technology*, *55*(20), 14069-14079.
- Leung, P., Wan, H., Billah, M., Cao, J., Ho, K., & Wong, C. K. (2014). Chemical and biological characterization of air particulate matter 2.5, collected from five cities in China. *Environmental Pollution*, *194*, 188-195.
- Li, N., Xia, T., & Nel, A. E. (2008). The role of oxidative stress in ambient particulate matter-induced lung diseases and its implications in the toxicity of

engineered nanoparticles. *Free radical biology and medicine*, *44*(9), 1689-1699.

- Lindberg, S., & Turner, R. (1988). Factors influencing atmospheric deposition, stream export, and landscape accumulation of trace metals in forested watersheds. *Water, Air, and Soil Pollution*, *39*, 123-156.
- Lippmann, M., Frampton, M., Schwartz, J., Dockery, D., Schlesinger, R., Koutrakis, P., Froines, J., Nel, A., Finkelstein, J., & Godleski, J. (2003). The US Environmental Protection Agency Particulate Matter Health Effects Research Centers Program: a midcourse report of status, progress, and plans. *Environmental Health Perspectives*, *111*(8), 1074-1092.
- Liu, H., Cao, C., Huang, J., Chen, Z., Chen, G., & Lai, Y. (2020). Progress on particulate matter filtration technology: basic concepts, advanced materials, and performances. *Nanoscale*, *12*(2), 437-453.
- Liu, L., Urch, B., Szyszkowicz, M., Evans, G., Speck, M., Van Huang, A., Leingartner, K., Shutt, R. H., Pelletier, G., & Gold, D. R. (2018). Metals and oxidative potential in urban particulate matter influence systemic inflammatory and neural biomarkers: A controlled exposure study. *Environment international*, *121*, 1331-1340.
- Manisalidis, I., Stavropoulou, E., Stavropoulos, A., & Bezirtzoglou, E. (2020). Environmental and health impacts of air pollution: a review. *Frontiers in public health*, *8*, 14.
- Matter, I. P. (2024). Health (PM2. 5 and PM10)| California Air Resources Board. In.
- Mazuryk, O., Stochel, G., & Brindell, M. (2020). Variations in reactive oxygen species generation by urban airborne particulate matter in lung epithelial cells—Impact of inorganic fraction. *Frontiers in chemistry*, *8*, 581752.
- Mazzoli-Rocha, F., Fernandes, S., Einicker-Lamas, M., & Zin, W. A. (2010). Roles of oxidative stress in signaling and inflammation induced by particulate matter. *Cell biology and toxicology*, *26*(5), 481-498.
- Moore, K. D., Wojcik, M. D., Martin, R. S., Marchant, C. C., Jones, D. S., Bradford, W. J., Bingham, G. E., Pfeiffer, R. L., Prueger, J. H., & Hatfield, J. L. (2015). Particulate-matter emission estimates from agricultural spring-tillage operations using LIDAR and inverse modeling. *Journal of Applied Remote Sensing*, *9*(1), 096066-096066.
- Mukherjee, A., & Agrawal, M. (2017). World air particulate matter: sources, distribution and health effects. *Environmental chemistry letters*, *15*, 283-309.
- Murphy, M. P., Bayir, H., Belousov, V., Chang, C. J., Davies, K. J., Davies, M. J., Dick, T. P., Finkel, T., Forman, H. J., & Janssen-Heininger, Y. (2022). Guidelines for measuring reactive oxygen species and oxidative damage in cells and in vivo. *Nature metabolism*, *4*(6), 651-662.
- Nelms, S., & Kutscher, D. (2022). Understanding the Fundamental Components of Sample Introduction for ICP-OES and ICP-MS.
- Ny, M. T., & Lee, B.-K. (2011). Size distribution of airborne particulate matter and associated metallic elements in an urban area of an industrial city in Korea. *Aerosol and Air Quality Research*, *11*(6), 643-653.
- Offor, I. F., Adie, G. U., & Ana, G. R. (2016). Review of particulate matter and elemental composition of aerosols at selected locations in Nigeria from 1985–2015. *Journal of Health and Pollution*, *6*(10), 1-18.
- Organization, W. H. (2021a). WHO global air quality guidelines. 2021. In.
- Organization, W. H. (2021b). *WHO global air quality guidelines: particulate matter (PM2. 5 and PM10), ozone, nitrogen dioxide, sulfur dioxide and carbon monoxide*. World Health Organization.
- Organization, W. H., & Organization, W. H. (2021). WHO Global Air Quality Guidelines: Particulate Matter (PM2. 5 and PM10). *Ozone, Nitrogen Dioxide, Sulfur Dioxide and Carbon Monoxide*, *1302*.
- Patel, P., & Aggarwal, S. G. (2022). On the techniques and standards of particulate matter sampling. *Journal of the Air & Waste Management Association*, *72*(8), 791-814.
- Pope 3rd, C. (1996). Particulate pollution and health: a review of the Utah valley experience. *Journal of exposure analysis and environmental epidemiology*, *6*(1), 23-34.
- Potter, N. A., Meltzer, G. Y., Avenbuan, O. N., Raja, A., & Zelikoff, J. T. (2021). Particulate matter and associated metals: A link with neurotoxicity and mental health. *Atmosphere*, *12*(4), 425.
- Pryor, J. T., Cowley, L. O., & Simonds, S. E. (2022). The physiological effects of air pollution: particulate matter, physiology and disease. *Frontiers in public health*, *10*, 882569.
- Pun, B. K., & Seigneur, C. (1999). Understanding particulate matter formation in the California San Joaquin Valley: Conceptual model and data needs. *Atmospheric Environment*, *33*(29), 4865-4875.
- Querol, X., Alastuey, A., Lopez-Soler, A., & Plana, F. (2000). Levels and chemistry of atmospheric particulates induced by a spill of heavy metal mining wastes in the Donana area, Southwest Spain. *Atmospheric Environment*, *34*(2), 239-253.
- Ruijrok, W., Davidson, C. I., & W. NICHOLSON, K. (1995). Dry deposition of particles. *Tellus B*, *47*(5), 587-601.
- Russell, A. G., & Brunekreef, B. (2009). A focus on particulate matter and health. In: ACS Publications.
- Shahpoury, P., Lelieveld, S., Srivastava, D., Baccarini, A., Mastin, J., Berkemeier, T., Celo, V., Dabek-Zlotorzynska, E., Harner, T., & Lammel, G. (2024). Seasonal Changes in the Oxidative Potential of Urban Air Pollutants: The Influence of Emission Sources and Proton-and Ligand-Mediated Dissolution of Transition Metals. *ACS Es&t Air*, *1*(10), 1262-1275.
- Sharma, M., Pandey, R., Maheshwary, M., Sengupta, B., Shukla, B., & Mishra, A. (2003). Air quality index and its interpretation for the city of Delhi. *International Journal of Energy for a Clean Environment*, *4*(3).
- Shen, J., Griffiths, P. T., Campbell, S. J., Utinger, B., Kalberer, M., & Paulson, S. E. (2021). Ascorbate oxidation by iron, copper and reactive oxygen species: Review, model development, and derivation of key rate constants. *Scientific reports*, *11*(1), 7417.
- Sokhi, R. S., Moussiopoulos, N., Baklanov, A., Bartzis, J., Coll, I., Finardi, S., Friedrich, R., Geels, C.,

Grönholm, T., & Halenka, T. (2021). Advances in air quality research–current and emerging challenges. *Atmospheric Chemistry and Physics Discussions*, *2021*, 1-133.

- Soleimanian, E., Taghvaee, S., Mousavi, A., Sowlat, M. H., Hassanvand, M. S., Yunesian, M., Naddafi, K., & Sioutas, C. (2019). Sources and temporal variations of coarse particulate matter (PM) in Central Tehran, Iran. *Atmosphere*, *10*(5), 291.
- Sousan, S., Pender, J., Streuber, D., Haley, M., Shingleton, W., & Soule, E. (2022). Laboratory determination of gravimetric correction factors for real-time area measurements of electronic cigarette aerosols. *Aerosol science and technology*, *56*(6), 517-529.
- Tacu, I., Kokalari, I., Abollino, O., Albrecht, C., Malandrino, M., Ferretti, A. M., Schins, R. P., & Fenoglio, I. (2021). Mechanistic insights into the role of iron, copper, and carbonaceous component on the oxidative potential of ultrafine particulate matter. *Chemical Research in Toxicology*, *34*(3), 767-779.
- Thompson, J. E. (2018). Airborne particulate matter: human exposure and health effects. *Journal of occupational and environmental medicine*, *60*(5), 392-423.
- Trejo-González, A. G., Riojas-Rodriguez, H., Texcalac-Sangrador, J. L., Guerrero-López, C. M., Cervantes-Martinez, K., Hurtado-Diaz, M., de la Sierra-de la Vega, L. A., & Zuñiga-Bello, P. E. (2019). Quantifying health impacts and economic costs of PM 2.5 exposure in Mexican cities of the National Urban System. *International journal of public health*, *64*, 561-572.
- Tyler, G., & Yvon, J. (1995). ICP-OES, ICP-MS and AAS Techniques Compared. *ICP Optical Emission Spectroscopy Technical Note*, *5*, 1-11.
- Utinger, B., Campbell, S. J., Bukowiecki, N., Barth, A., Gfeller, B., Freshwater, R., Rüegg, H.-R., & Kalberer, M. (2023). An automated online field instrument to quantify the oxidative potential of aerosol particles via ascorbic acid oxidation. *Atmospheric Measurement Techniques*, *16*(10), 2641-2654.
- Vörösmarty, M., Uzu, G., Jaffrezo, J.-L., Dominutti, P., Kertész, Z., Papp, E., & Salma, I. (2023). Oxidative potential in rural, suburban and city centre atmospheric environments in central Europe. *Atmospheric Chemistry and Physics*, *23*(22), 14255-14269.
- Watson, J. G., Zhu, T., Chow, J. C., Engelbrecht, J., Fujita, E. M., & Wilson, W. E. (2002). Receptor modeling application framework for particle source apportionment. *Chemosphere*, *49*(9), 1093-1136.
- Weber, S., Uzu, G., Favez, O., Borlaza, L. J. S., Calas, A., Salameh, D., Chevrier, F., Allard, J., Besombes, J.-L., & Albinet, A. (2021). Source apportionment of atmospheric PM 10 oxidative potential: synthesis of 15 year-round urban datasets in France. *Atmospheric Chemistry and Physics*, *21*(14), 11353-11378.
- Yamamoto, S., Louis, V., Sié, A., & Sauerborn, R. (2014). Biomass smoke in Burkina Faso: what is the relationship between particulate matter, carbon monoxide, and kitchen characteristics? *Environmental Science and Pollution Research*, *21*, 2581-2591.
- Zhang, L., Ou, C., Magana-Arachchi, D., Vithanage, M., Vanka, K. S., Palanisami, T., Masakorala, K., Wijesekara, H., Yan, Y., & Bolan, N. (2021). Indoor particulate matter in urban households: sources, pathways, characteristics, health effects, and exposure mitigation. *International journal of environmental research and public health*, *18*(21), 11055.
- Zhang, Z.-H., Hartner, E., Utinger, B., Gfeller, B., Paul, A., Sklorz, M., Czech, H., Yang, B. X., Su, X. Y., & Jakobi, G. (2021). Are reactive oxygen species (ROS) a suitable metric to predict toxicity of carbonaceous aerosol particles? *Atmospheric Chemistry and Physics Discussions*, *2021*, 1-29.
- Zhu, Y., Smith, T. J., Davis, M. E., Levy, J. I., Herrick, R., & Jiang, H. (2011). Comparing gravimetric and real-time sampling of PM2. 5 concentrations inside truck cabins. *Journal of occupational and environmental hygiene*, *8*(11), 662-672.